ORIGINAL RESEARCH

Effects of Aging on Cardiac Oxidative Stress and Transcriptional Changes in Pathways of Reactive Oxygen Species Generation and Clearance

Farhan Rizvi, PhD; Claudia C. Preston (iD), MD; Larisa Emelyanova (iD), PhD; Mohammed Yousufuddin, MD; Maria Viqar, MD; Omar Dakwar, MS; Gracious R. Ross, PhD; Randolph S. Faustino, PhD; Ekhson L. Holmuhamedov, PhD; Arshad Jahangir (iD), MD

BACKGROUND: Age-related heart diseases are significant contributors to increased morbidity and mortality. Emerging evidence indicates that mitochondria within cardiomyocytes contribute to age-related increased reactive oxygen species (ROS) generation that plays an essential role in aging-associated cardiac diseases.

METHODS AND RESULTS: The present study investigated differences between ROS production in cardiomyocytes isolated from adult (6 months) and aged (24 months) Fischer 344 rats, and in cardiac tissue of adult (18–65 years) and elderly (>65 years) patients with preserved cardiac function. Superoxide dismutase inhibitable ferricytochrome c reduction assay (1.32 ± 0.63 versus 0.76 ± 0.31 nMol/mg per minute; $P=0.001$) superoxide and H_2O_2 production, measured as dichlorofluorescein diacetate fluorescence (1646 ± 428 versus 699 ± 329, $P=0.04$), were significantly higher in the aged versus adult cardiomyocytes. Similarity in age-related alteration between rats and humans was identified in mitochondrial-electron transport chain-complex-I-associated increased oxidative-stress by MitoSOX fluorescence (53.66 ± 18.58 versus 22.81 ± 12.60; $P=0.03$) and in 4-HNE adduct levels (187.54 ± 54.8 versus 47.83 ± 16.7 ng/mg protein, $P=0.0063$), indicative of increased peroxidation in the elderly. These differences correlated with changes in functional enrichment of genes regulating ROS homeostasis pathways in aged human and rat hearts. Functional merged collective network and pathway enrichment analysis revealed common genes prioritized in human and rat aging-associated networks that underlay enriched functional terms of mitochondrial complex I and common pathways in the aging human and rat heart.

CONCLUSIONS: Aging sensitizes mitochondrial and extramitochondrial mechanisms of ROS buildup within the heart. Network analysis of the transcriptome highlights the critical elements involved with aging-related ROS homeostasis pathways common in rat and human hearts as targets.

Key Words: cardiac aging ■ electron transport chain ■ gene expression ■ oxidative stress ■ reactive oxygen species

Reactive oxygen species (ROS) such as superoxide anion (O_2^{-}) and hydrogen peroxide (H_2O_2) are continuously generated at low levels within the cell and play an essential role in various physiological processes; during stress they may contribute to cell injury and death.[1-4] An increased ROS production rate has been implicated in aging and age-related changes in the mammalian heart, leading to gradual functional impairment,[5,6] including reduced tolerance to stress and cellular energetic reserves, and predisposing cells to injury.[7-10] The rate of aging-associated decline in function varies by species as well as by organ within the

CLINICAL PERSPECTIVE

What Is New?

- Selective downregulation in the activity of electron transport chain complex I involved in superoxide generation is the common link in reactive oxygen species production in aging rat and human myocardium.
- Network analysis of the transcriptome highlights similar mechanisms and pathways involved in aging rats and humans with ERK1/2 linking to electron transport chain complex I as a common signaling pathway in the aging heart.

What Are the Clinical Implications?

- Recognizing regulators of reactive oxygen species homeostasis and its downstream players altered by aging may identify targets that can be selectively intervened on to prevent aging-associated electrical or mechanical myocardial dysfunction, such as atrial fibrillation and heart failure, prevalent in the elderly.

Nonstandard Abbreviations and Acronyms

AU	arbitrary units
ETC	electron transport chain
IPA	Ingenuity Pathway Analysis
LCM	low-calcium medium
ROS	Reactive oxygen species

same species and is influenced by genetic and environmental factors[11-14] with deleterious consequences, increasing predisposition to ischemic heart disease, cardiomyopathy, and cardiac arrhythmias.[6,12,14] The relative contribution of enhanced production versus reduced clearance of ROS within the cytoplasm and mitochondria is not fully characterized, and the impact of aging versus disease on these pathways in humans is not well defined. To address this, we compared age-related alteration in the sensitivity of myocardial tissue to stress-related alteration in oxidant production in cardiomyocytes from disease-free young and aged Fischer 344 rats, an established model of aging, and in human cardiac tissue from adult and aged patients undergoing cardiac surgery. We also assessed overall change in the expression of genes encoding for pathways of ROS production and clearance in young and aged rat hearts and in young and aged patients undergoing cardiac surgery. From aged rat and human hearts, we identified shared networks and nodes that are important for regulating oxidative stress and that are altered with aging in both rats and humans. This

information provides novel insight into potential targets involved in the responsiveness of the elderly heart to stress that could be manipulated to prevent aging-associated deterioration in heart function.[15]

METHODS

Human Sample Selection

Atrial appendage tissue was harvested from adult (18–65 years) and aged (>65 years) patients undergoing elective open-heart surgery for coronary artery disease, and tissue from those who met inclusion and exclusion criteria was used for the analysis of the study. The baseline clinical characteristics of these patients is summarized in Table S1. Patients with congenital, structural, or functional atrial disease—including persistent or permanent atrial fibrillation—or class III/IV heart failure, those requiring inotropic support, and those with moderate/severe mitral valve disease were excluded. The research study was conducted following the Declaration of Helsinki for experiments relating to humans. The study was approved by the Aurora Health Care Institutional Review Board for human subject research, written informed consent was obtained from all subjects, and all patients' privacy rights were observed. The data that support the findings of this study are available from the corresponding author upon reasonable request.

Processing of Human Cardiac Samples

After clamping and removal of the atrial appendage, the tissue was immediately transferred into ice-cold Dulbecco's phosphate-buffered saline. Fat and connective tissue were removed from the biospecimen, and the muscle tissue was freshly used for myofiber isolation or frozen in liquid nitrogen (N2) and stored at −80°C for future use. A total of 47 patients' samples were used in this research for the various expressional and functional studies (OXPHOS functional analysis, 4-HNE protein adducts, western blot, or genetic analysis). Tissue was collected immediately after removal from the patient and processed within 10 to 15 minutes. If any delay occurred in collection or storage, the tissue was not used for the study.

Experimental Animals and Design

Animal experiments were approved by the Institutional Animal Care and Use Committee of the Mayo Clinic College of Medicine and conformed to the National Institutes of Health *Guide for the Care and Use of Laboratory Animals* (NIH Pub. No. 85-23, 1996). The young adult (6 months old) and aged (24 months old) male Fischer 344 rats were used for our aging-related studies.[16-18] Young and aged rats were acquired from the National Institute on Aging (NIA) colonies[19] and

were housed in a temperature-controlled room (22–23°C) with a 12:12-hour light-dark cycle and fed with tap water and Purina Laboratory Chow (No. 5001) ad libitum. Rats were euthanized with intraperitoneal sodium pentobarbital (50 mg/kg) before thoracotomy and heart dissection. In a set of parallel experiments in young adult and aged rats, we determined (1) $O_2^{.-}$ generation by the mitochondria isolated from ventricles and (2) steady-state and ouabain-stressed H_2O_2 production in isolated cardiomyocytes.

Isolation of Cardiomyocytes From Rat Hearts

Cardiomyocytes were isolated from the hearts of young adult (n=5) and aged (n=5) rats, as described previously.[20] In brief, the procedure comprises three main steps: (1) dissection and sequential retrograde perfusion of the heart at 37°C, firstly, with Tyrode's buffer (137 mmol/L NaCl, 10 mmol/L glucose, 10 mmol/L HEPES, 5.4 mmol/L KCl, 1 mmol/L $MgCl_2$, and 2 mmol/L $CaCl_2$) for 10 minutes; secondly, with a "low-calcium" medium (LCM) containing 100 mmol/L NaCl, 50 mmol/L taurine, 20 mmol/L glucose, 10 mmol/L KCl, 10 mmol/L HEPES, 5 mmol/L $MgSO_4$, and 1.2 mmol/L KH_2PO_4 and supplemented with 0.13 mmol/L $CaCl_2$ and 2.1 mmol/L EGTA for 2 minutes; and finally, with LCM supplemented with 1% bovine serum albumin (BSA), 0.2 mmol/L $CaCl_2$, collagenase (type II, 22 U/mL; Worthington) and pronase (100 µg/mL; Serva) for 15 minutes; (2) removal of atria and mincing of the ventricular tissue into small pieces before incubation in the enzyme solution with gentle stirring at 37°C for 15 minutes; (3) isolation of intact cardiomyocytes by serial centrifugation and washing of the pellet in LCM supplemented with 0.2 mmol/L $CaCl_2$ (wash) followed by suspension in the wash solution.[21]

Isolation of Mitochondria From the Heart

Mitochondria were isolated from the myocardium of young adult (n=5) and aged (n=5) rats as previously described.[22] In summary, ventricles were excised from the rat heart, sliced into fine pieces, suspended in an isolation buffer containing (in millimoles) sucrose 50, mannitol 20, KH_2PO_4 5, EGTA 1, and Mops 5 (pH 7.3, adjusted with KOH) with 0.2% BSA, and then homogenized to isolate mitochondria. The mitochondrial fraction was obtained by differential centrifugation, washed, and suspended in isolation buffer free of EGTA and BSA and kept on ice for the experiment.[6]

Measurement of $O_2^{.-}$ Generation by the Mitochondria

The rate of $O_2^{.-}$ generation was measured as superoxide dismutase (SOD)-inhibitable reduction of acetylated ferricytochrome c. The reaction mixture contained 0.1 mol/L potassium phosphate buffer (pH 7.4), 7.2 µmol/L acetylated cytochrome c, 2 µmol/L antimycin A, 6 µmol/L rotenone, 10 mmol/L succinate, and 20 to 30 µg/mL mitochondrial protein with glutamate/malate as substrates; 100 units of SOD/mL was added to the reference cuvette. The cytochrome c reduction was recorded at 37°C for 10 minutes by monitoring absorbance at 550 to 540 nm in the presence or absence of SOD. The increase in absorbance at 550 to 540 nm is caused by the formation of stoichiometric ferrous cytochrome c. The production of $O_2^{.-}$ was estimated with the extinction coefficient of 19.0 $mM^{-1}\cdot cm^{-1}$ and expressed as a mean of multiple experiments.[23-25]

H_2O_2 Production Within Isolated Cardiomyocytes

H_2O_2 production was estimated using ROS-sensitive fluorophore, 2′, 7′-dichlorofluorescein diacetate (DCFDA) (Molecular Probes, Eugene, OR). The freshly isolated cardiomyocytes were placed in collagen-coated glass Petri dishes (Mat Tek Corp., Ashland, MA) at room temperature. The cells were incubated for 45 minutes with DCF at 37°C. The DCFDA solution was removed, and the cells were washed with serum-free medium. Fluorescence intensity of DCF was measured at 585 nm emission when excited at 488 nm by an LSM 510 laser-scanning confocal microscope. Confocal microscopic images were acquired every minute from 0 to 10 minutes using incorporated software (Carl Zeiss Inc., Thornwood, NY). Cardiomyocytes were then stressed with 30, 100, and 300 µmol/L ouabain (Sigma) or vehicle (DMSO 1%) for 15 minutes at room temperature. Following initial ouabain exposure, cardiomyocytes were loaded with the H_2O_2-selective dye DCFDA (4 µmol/L; Molecular Probes) for 15 minutes to detect ROS generation. Confocal images were acquired with an LSM 510 laser scanning confocal microscope using incorporated software. The single-excitation, single-emission, fluorescent probe DCFDA was excited using the 568 nm line of the Ar/Kr laser, and emitted fluorescence was filtered through long-pass filter settings (LP 585). Confocal microscopic images were acquired every minute from 0 to 10 minutes after treatment with ouabain, and data were analyzed using LSM 400 software (Zeiss).

Determination of 4-Hydroxynonenal Protein Adducts

An OxiSelect HNE adduct competitive ELISA commercial kit (Cat #STA-838, Cell Biolabs, INC, San Diego, CA) was used to measure the level of 4-HNE in cardiac tissue homogenate. Human cardiac tissue (n=41) homogenate prepared in ice-cold phosphate-buffered

saline with 0.1% BSA was centrifuged for 10 minutes at 10 000g, and the 4-hydroxynonenal (4-HNE) level was assessed in the supernatant as per the kit's guidelines.

Mitochondrial Superoxide Production in Permeabilized Human Cardiac Myofibers

Superoxide production in the cardiac myofibers was determined as previously described.[6] Atrial appendage tissue soaked in ice-cold buffer containing (in mmol/L) 7.23 K_2EGTA, 2.77 CaK_2EGTA, 20 imidazole, 20 taurine, 5.7 ATP, 14.3 phosphocreatine, 6.56 $MgCl_2 \cdot 6H_2O$, and 50 MES (pH 7.1) was cut into small strips and incubated with collagenase type I for 30 to 45 minutes at 4°C. Connective tissue and fat were then removed, and the fibers mechanically separated along the longitudinal axis and permeabilized with saponin (30–50 μg/mL) for 30 minutes at 4°C. Following permeabilization, myofibers were washed in an ice-cold buffer containing (in mmol/L) 110 K-MES (pH 7.4), 35 KCl, 1 EGTA, 5 KH_2PO4, 3 $MgCl_2 \cdot 6H_2O$, and 0.02 blebbistatin with 5 mg/mL BSA. The myofibers remained in the ice-cold buffer, supplemented with 100 μmol/L ADP, 5 mmol/L glucose, and 1 U/mL hexokinase to keep mitochondria in an energized and phosphorylating state,[26] until used for measuring mitochondrial superoxide production. The level of superoxide production in the myofibers was determined as a change in fluorescence intensity of MitoSOX Red (λex/λem=510/580; Cat #M36008, Thermo Fisher Scientific, Waltham, MA), a mitochondrial superoxide-sensitive indicator, in response to 10 μmol/L antimycin A (Cat #A8674, Sigma-Aldrich, St. Louis, MO)[6,27] exposure by time-lapse laser scanning confocal fluorescence microscopy. Images were detected in an Olympus FV1200 confocal microscope (Olympus, Tokyo, Japan). The change in MitoSOX Red fluorescence intensity before and after antimycin A addition was quantified to measure the difference in the superoxide production.[6,27]

Mitochondrial Complex (I–V) Enzymatic Activity

Frozen human cardiac tissue sample (30–50 mg) was homogenized in an ice-cold buffer (1:20 w/v) containing (in mmol/L) 100 KCl, 5 $MgCl_2$, 2 EGTA, and 50 Tris/HCl (pH 7.5), using an OMNI GLH-115 Polytron homogenizer (OMNI International). The supernatant collected after centrifuging the homogenates at 1000g for 15 minutes at 4°C was used to measure the functional activity of mitochondrial electron transport chain (ETC) complexes as reported earlier.[6,14]

RNA Extraction

Freshly isolated human or rat cardiac tissue was snap-frozen in liquid nitrogen before storage at −80°C until subsequent processing for gene expression analysis by microarray or by reverse transcription (q) polymerase chain reaction (PCR). Frozen human or rat tissue was homogenized in TRIzol (Invitrogen Corp., Carlsbad, CA) using a PELLET PESTLE motor homogenizer (Kimble-Kontes, Vineland, NJ). Total RNA was extracted using a TRIzol Reagent kit according to the manufacturer's specifications.[6,8] Further purification was carried out using RNeasy Mini Kit (QIAGEN Inc., Valencia, CA). RNA concentrations were determined using the Infinite 200 NanoQuant (Tecan Group Ltd., Männedorf, Switzerland), and quality/integrity was assessed by Agilent 2100 Bioanalyzer (Affymetrix, Santa Clara, CA).

Reverse Transcription (q) PCR Assay of Target mRNA

Equal amounts of RNA isolated from each human cardiac tissue sample, n=7 adults (age ≤65 years) and n=10 aged (age >65 years), were reverse-transcribed to cDNA using a miScript RT II kit (Qiagen). Quantitative PCRs were performed in an LC480 real-time PCR system (Roche, Risch-Rotkreuz, Switzerland) using SYBR Green PCR Master Mix (Thermo Fisher Scientific). Details of gene-specific primer sequences used in this study are listed in Table S2. The qPCR reactions were performed in triplicate for all samples. Relative mRNA expression (ΔCq) normalized to reference B2M and 18s RNA expression were determined using LightCycler 480 Software.

Western Blot Analysis

Frozen human cardiac tissue (n=5 adult and n=5 aged) was homogenized in RIPA lysis buffer (Abcam, Cambridge, MA) with protease inhibitor cocktail freshly added (Millipore Sigma). Protein lysates (15 μg) were separated on NuPAGE precast 4% to 12% Bis-Tris gel (Thermo Fisher Scientific) and transferred to polyvinylidene difluoride membranes (Thermo Fisher Scientific). Western blotting was performed using primary anti-SOD1 (Cat #ab13498; Abcam), anti-SOD2 (Cat #ab13194; Abcam), and anti-β-tubulin (Cat #2148; Cell Signaling).

Bioinformatics: Functional Enrichment Analysis and Gene Target Prioritization

The Gene Ontology (GO) consortium website (http://geneontology.org), via its AmiGO 2 search browser, was used to determine all genes associated with ROS metabolic processes in humans (website accessed February 29, 2020). Venn diagrams were used to intersect this ROS list with our previously published datasets from human (GSE173608) and rat (GSE173360) aged hearts to identify ROS-associated candidates.

Functional deconvolution of mitochondrial-related and extramitochondrial genes involved in ROS metabolism from human and rat aged hearts was performed via Ingenuity Pathway Analysis (IPA; Qiagen, Germantown, MD; last accessed for analysis June 16, 2020). IPA was used to determine prioritized canonical pathways, pathway activity analysis (prediction of functional pathways), and mapping of functional gene networks defined by the differentially expressed genes in aged human and rat hearts. The significance of canonical functional pathways, calculated by Benjamini-Hochberg multiple testing correction (corrected P value=P [Corr]), indicates the probability of association between a gene/target and a specific functional pathway. Pathway activity analysis determines whether a canonical pathway is activated (increased) or inhibited (decreased), predicted by a z-score algorithm used to compare the uploaded gene list with the canonical pathway patterns and displayed by colored bar charts indicating their functional pathway activation z-scores. The highest priority network scores were determined, and the Molecule Activity Predictor Analysis (IPA module) was used to predict activation or inhibition of non-focused neighboring molecules within the prioritized functional network in human and rat datasets. All gene interactions from networks, prioritized, and merged networks were exported from IPA for use in Cytoscape (v3.7.1; https://cytoscape.org/) for further network analysis (last accessed for analysis June 15, 2020). Prioritization of gene targets was achieved through graph theory analysis tools (network metrics: neighborhood connectivity, betweenness, and closeness centralities) within Cytoscape.

Statistical Analysis

The statistical analysis was performed using SAS software (version 9.2, SAS Institute, Cary, NC) and GraphPad Prism (version 8, GraphPad Software, San Diego, CA). The differences between adult and aged rats were assessed by Student t test. Comparison of the aged and adult humans was performed using the t test for normally distributed variables or the nonparametric Kruskal-Wallis test for the variables that deviate from the normal distribution. Mean±standard deviation was applied to describe quantitative variables, and percentages were used for qualitative variables. The Kolmogorov-Smirnov test was used to evaluate the normality of continuous variable distribution. Simple linear regression was performed to investigate the relationship between variables. The number of patient samples used for each experiment is detailed in Table S3. Bioinformatics analysis for canonical functional pathways significance was calculated using false discovery rate, Benjamini-Hochberg multiple testing correction (corrected P value=P [Corr]). Probability

value (P) and P (Corr) <0.05 were considered significant. The rates of O_2^- and H_2O_2 production were expressed as the mean and SEM.

RESULTS

Aging Alters the Functional Enrichment of Genes Involved in ROS Metabolism and Depicts Mitochondrial Function and Oxidative Phosphorylation as the Most Prioritized Pathways

Our previous work showed gene expression changes in mitochondrial-related genes in both human and rat aging hearts compared to adult hearts.[8,14] Some of these genes coding for mitochondrial localized proteins are involved in ROS metabolism, including ROS production and clearance. In both rat and human heart aging, associated changes in mitochondrial and extramitochondrial pathways for ROS production and clearance were observed. These changes were predominantly involved in oxidative stress pathways and significantly reduced expression of subunits involved in electron transport chain complex I. The species-independent alteration in genes common to both rats and humans with aging is summarized in Table S4.

Statistically significant genes from this dataset were intersected with ROS metabolism genes (n=285) extracted from the GO consortium website (www.geneo ntology.org/docs/go-consortium) to identify the ROS-associated changes in the aging heart (Figure 1A and 1B, Table S4). In human myocardium, out of the 832 differentially expressed genes in the aged versus adult heart, 35 genes (4.2%) were involved in ROS homeostasis, with 27 (77%) downregulated and 8 (23%) upregulated. These 35 differentially expressed genes in human myocardium are 14% of the total ROS-associated genes present within the Gene Ontology consortium (Figure 1A). Similarly, in the aged rat heart, there were 916 differentially expressed genes, out of which 47 (5.1%) were involved in ROS metabolism; 39 of these genes (83%) were downregulated and 8 (17%) upregulated. Out of the total 250 ROS-metabolism-associated genes reported in the Gene Ontology consortium, 47 (18.8%) genes were differentially expressed in the aged rat heart (Figure 1B). In both aged human and rat datasets, the majority of genes involved in ROS homeostasis were downregulated. Functional pathway enrichment analysis from IPA revealed that "mitochondrial dysfunction," "oxidative phosphorylation," and "sirtuin signaling pathway" were the three prioritized functions in the human and rat aging heart datasets (Figure 1C and 1D). The human dataset exposed three significant canonical pathways ("mitochondrial dysfunction," "oxidative phosphorylation," and "sirtuin
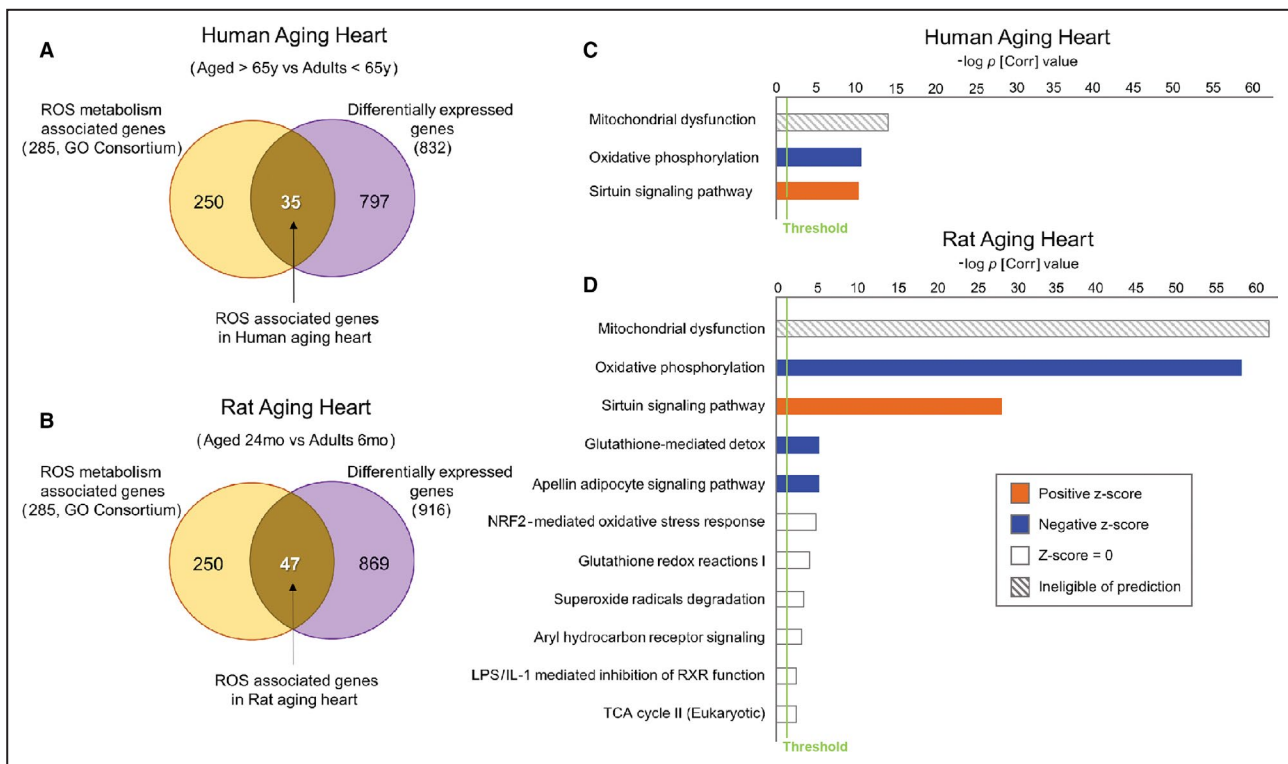
Figure 1.   ROS-associated functional pathways changes in aging human and Fischer 344 rat hearts.
A, Out of the 832 differentially expressed genes (DEG) in aged compared to adult hearts, 35 genes (4.2%) were associated with ROS metabolism, with 27 genes downregulated and 8 upregulated in the human aged heart. **B**, In the aging rat heart, out of 916 DEGs we found 47 (5.1%) ROS-metabolism-associated genes (39 downregulated, 8 upregulated). **C**, Functional and pathway analysis exposed three significant canonical pathways enriched in the human dataset: "mitochondrial dysfunction" (white/gray pattern=ineligible of pathway prediction), "oxidative phosphorylation" (blue=predicted decrease in activity of pathway), and "sirtuin signaling pathways" (orange=predicted increase in activity). Threshold was set at P [Corr] <0.05 (green line). **D**, ROS-pathway-associated genes from aged rats enriched distinctive and significant functional categories that were similar in rats and humans for the top three canonical pathways, with stronger significance reported for the former. Furthermore, "glutathione-mediated detox" and "apelin adipocyte signaling pathway" also predicted decrease in activity (blue bars). Six other functional pathways were significantly enriched; however, they showed neutral predicted activity. (For details, see Methods and Materials). IPA indicates Ingenuity Pathways Analysis; P [Corr], Corrected P value including multiple testing correction (Benjamini Hochberg false discovery rate); and ROS, reactive oxygen species.

signaling pathway"; Figure 1C). The pathway activity analysis module from IPA predicted a decrease in the activity of the "oxidative phosphorylation" pathway (−log P [Corr]=9.85; Figure 1C), whereas the "sirtuin signaling pathway" was predicted to be increased (−log P [Corr]=9.54; Figure 1C). However, IPA was not able to discern a significant predictive pattern for "mitochondrial dysfunction" (−log P [Corr]=13.16; Figure 1C). In the aging rat heart, ROS-pathway-associated genes enriched distinctive and significant functional categories (Figure 1D). The top three canonical pathways, and the pathway activity analysis, matched those identified in the aged human heart, however, with much higher statistical significance: "mitochondrial dysfunction" (−log P [Corr]=61.50; Figure 1D), "oxidative phosphorylation" (−log P [Corr]=58.14; Figure 1D), and "sirtuin signaling pathway" (−log P [Corr]=20.04; Figure 1D). Furthermore, "glutathione-mediated detox" and "apelin adipocyte signaling pathway" showed a predicted

decrease in pathway activity (−log P [Corr]=5.25, and −log P [Corr]=5.23, respectively; Figure 1D). Six other functional pathways, namely "NRF2-mediated oxidative stress response," "glutathione redox reaction 1," "superoxide radical degradation," "aryl hydrocarbon receptor signaling," "LPS/IL-1-mediated inhibitor RXR function," and "TCA cycle II" were significantly altered but showed a neutral z-score of zero or close to zero, meaning the activity of the pathways was predicted to neither be increased nor decreased.

Further functional pathway activity analysis was used to determine predictive activity patterns of categorical functions associated with the "free radical scavenging" function in both the human and rat datasets (Table). The human dataset identified four functions associated with metabolism, synthesis, and generation of ROS that showed a positive z-score trend but no significant predictive activity (P [Corr] <0.01, z-score >0.5; Table). In comparison to the human dataset, the

Table.   Predicted Activation and Inhibition of Categorical Annotations Within the "Free Radical Scavenging" Function

Free Radical Scavenging Function	P [Corr]	z-Score	Gene Associated With Function
Human ROS			
Metabolism of ROS	<0.0001	0.864	ATG5, ATP7A, BNIP3, CAV1, CYB5R4, FOXO3, PINK1, UQCRC2
Synthesis of ROS	0.0006	0.864	ATG5, BNIP3, CAV1, FOXO3, PINK1, UQCRC2
Generation of ROS	0.0007	0.555	BNIP3, CAV1, PINK1, UQCRC2
Production of ROS	0.0075	0.507	ATG5, CAV1, FOXO3, PINK1
Generation of hydrogen peroxide	0.0014	…	CAV1, PINK1
Scavenging of hydrogen peroxide	0.0030	…	FOXO3
Quantity of ROS	0.0069	…	ATG5, FOXO3, NNT
Rat ROS			
Production of ROS	<0.0001	2.205*	COX8A, CYBB, NDUFS1, SOD1, SOD2, TXN2, UQCRFS1, XDH
Production of superoxide	<0.0001	2.190*	CYBB, SOD1, SOD2, TXN2, XDH
Synthesis of ROS	<0.0001	2.128*	COX5B, COX6A2, COX8A, CYBB, NDUFS1, SDHC, SOD1, SOD2, TXN2, UQCRFS1, XDH
Formation of ROS	<0.0001	1.969	COX6A2, CYBB, SOD2, XDH
Quantity of ROS	<0.0001	1.948	CYBB, GSTA1, PRDX5, SOD1, SOD2, TXN2, XDH
Quantity of superoxide	<0.0001	1.447	CYBB, SOD1, SOD2, TXN2, XDH
Metabolism of ROS	<0.0001	1.186	COX5B, COX6A2, COX8A, CYBB, GPX3, GSTA4, NDUFS1, PRDX5, SDHC, SOD1, SOD2, TXN2, UQCRFS1, XDH
Generation of superoxide	<0.0001	1.109	CYBB, SOD1, SOD2, XDH
Generation of ROS	<0.0001	0.906	COX5B, CYBB, SDHC, SOD1, SOD2, UQCRFS1, XDH
Quantity of hydrogen peroxide	<0.0001	0.762	PRDX5, SOD1, SOD2, TXN2
Accumulation of ROS	<0.0001	0.600	CYBB, NDUFS1, PRDX5, SDHC, SOD1, SOD2
Metabolism of hydrogen peroxide	<0.0001	−1.955	CYBB, GPX3, PRDX5, SOD1, SOD2, UQCRFS1
Modification of ROS	<0.0001	−1.966	GSTA4, PRDX5, SOD1, SOD2
Accumulation of hydrogen peroxide	<0.0001	…	NDUFS1, PRDX5, SOD1, SOD2
Detoxification of ROS	<0.0001	…	GSTA4, SOD1, SOD2
Modification of hydrogen peroxide	<0.0001	…	PRDX5, SOD1, SOD2
Conversion of superoxide	<0.0001	…	SOD1, SOD2
Metabolism of superoxide	<0.0001	…	CYBB, SOD1, SOD2
Accumulation of superoxide	<0.0001	…	NDUFS1, SOD2
Reduction of superoxide	<0.0001	…	SOD1, SOD2
Degradation of hydrogen peroxide	<0.0001	…	GPX3, PRDX5, SOD1
Conversion of hydrogen peroxide	<0.0001	…	SOD1, SOD2
Biosynthesis of hydrogen peroxide	0.0001	…	CYBB, SOD1, SOD2, UQCRFS1
Removal of superoxide	0.0003	…	SOD1, SOD2
Formation of superoxide	0.0005	…	CYBB, SOD2
Quantity of lipid peroxide	0.0007	…	SOD1, XDH
Catabolism of hydrogen peroxide	0.0009	…	GPX3, PRDX5
Peroxidation of superoxide	0.0020	…	SOD1
Hyperproduction of superoxide	0.0020	…	CYBB
Generation of hydrogen peroxide	0.0026	…	SOD1, UQCRFS1

(Continued)

Table 1. Continued

Free Radical Scavenging Function	P [Corr]	z-Score	Gene Associated With Function
Breakdown of hydrogen peroxide	0.0040	…	SOD1
Detoxification of monohydroperoxy-linoleic acid	0.0040	…	GSTA4
Reduction of monohydroperoxy-linoleic acid	0.0061	…	GSTA4
Clearance of ROS	0.0121	…	SOD2
Production of hydrogen peroxide	0.0128	…	SOD1, SOD2
Reduction of hydrogen peroxide	0.0201	…	PRDX5

Using the Pathway Activity Analysis module from Ingenuity Pathways Analysis (IPA), we depict here the functional annotations with inferred activation (z-score >0) or inhibition (z-score <0) metrics along with corrected P value (P [Corr]) and gene names of molecules associated with each functional annotation. Both rat and human cardiac transcriptomes were used for this analysis. The human ROS dataset depicted four functions associated with generation and/or accumulation of ROS which showed a positive z-score trend, however, no significant predictive activity. In the rat ROS dataset, three functions were predicted to be activated in the rat ROS list: production of ROS, production of superoxide and synthesis of ROS (bold and z-scores highlighted with *). Moreover, eight other functions associated with generation and/or accumulation of ROS also had a positive z-score and two functions associated with ROS clearance and metabolism had a negative z-score, but they did not reach significant predictive threshold. P (Corr)=corrected P value with Benjamini-Hochberg false discovery rate. ROS indicates reactive oxygen species.

rat dataset did elicit predictive activity on some functions. The following functions were predicted to have a significant increase in activity within the rat dataset: "production of reactive oxygen species" (COX8A, CYBB, NDUFS1, SOD1, SOD2, TXN2, UQCRFS1, and XDH), "production of superoxide," with five genes associated with this functional term (CYBB, SOD1, SOD2, TXN2, and XDH), and "synthesis of reactive oxygen species" (COX5B, COX6A2, COX8A, CYBB, NDUFS1, SDHC, SOD1, SOD2, TXN2, UQCRFS1, and XDH; P [Corr] <0.0001, z-score >2.0; Table). Moreover, the other five terms related to metabolism and generation of ROS elicited z-scores above 1 but did not reach the threshold for activity prediction (Table).

Aging Is Associated With Alteration of Gene Expression Encoding for Mitochondrial ROS Production and Clearance Pathways

Figure 2 summarizes the statistically significant alteration in the expression of genes encoding for proteins involved in ROS production and clearance pathways in human (Figure 2A) and rat hearts (Figure 2B). The significant affect associated with the aged human heart was seen on complex I of the ETC, involved in the production of ROS, with downregulation of five subunits (NDUFA6, NDUFA9, NDUFB5, NDUFAB8, and NDUFS2) and upregulation of two complex assembly factors (NDUFAF5 and NDUFAF6) (Figure 2A). GLRX2, GLRX3, and PRDX4, which are involved in the clearance of ROS, were downregulated in the human aged heart, whereas TXNDC15 was upregulated. A similar change was seen in the aged rat hearts, with complex I having the majority of changes (13 genes downregulated; Figure 2B). Of note, some common genes were altered in both humans and rats, while other genes were unique to the rat myocardium

(Figure 2A and 2B; Table S4). Both NOX2 (1.6-fold; P=0.016) and XDH (1.4-fold; P=0.027; Table S4), two major enzymes involved in extramitochondrial superoxide production, were significantly upregulated in the rat heart but not significantly different between the adult and aged human myocardium. Table S4 summarizes the information on the differentially expressed subunits of the mitochondrial ETC as well as extramitochondrial ROS production and clearance and other ROS metabolism pathways along with fold change and their P values. In the mitochondrial ROS clearance pathway, significant differences were present between rat and human aging myocardium: in rat myocardium, GPX3 (1.6-fold; P<0.005), GTSA1 (2.6-fold; P<0.001), PRDX4 (1.3-fold; P=0.028), and TXNRD3 (2.2-fold; P<0.001) were upregulated and others (PRDX5, SOD1, SOD2, TXN2) were downregulated; in human myocardium, only downregulation of the genes involved in mitochondrial ROS clearance was observed (Figure 2A and 2B; Table S4). Differences also were present between rat and human hearts in their extramitochondrial ROS generation and clearance pathways.

To correlate changes in the gene expression of proteins involved in mitochondrial ROS production, activities of individual ETC complexes were determined in myocardial tissue from adult and aged patients (Figure 2C). ETC complex I activity, as determined by rotenone-sensitive reduction of ubiquinone-1, was significantly reduced in the elderly compared to adult (73.61±33.02 versus 111.4±42.76 nmol/min per mg protein, respectively, P=0.039; Figure 2C), similar to previously reported findings.[8,14] The functional activities of the remaining four OXPHOS complexes in humans were not significantly altered by age (complex II, P=0.2672; complex III, P=0.6216; complex IV, P=0.5216; complex V, P=0.3912; Figure 2C), a finding similar to that in aged rat and human myocardium.[8,14]
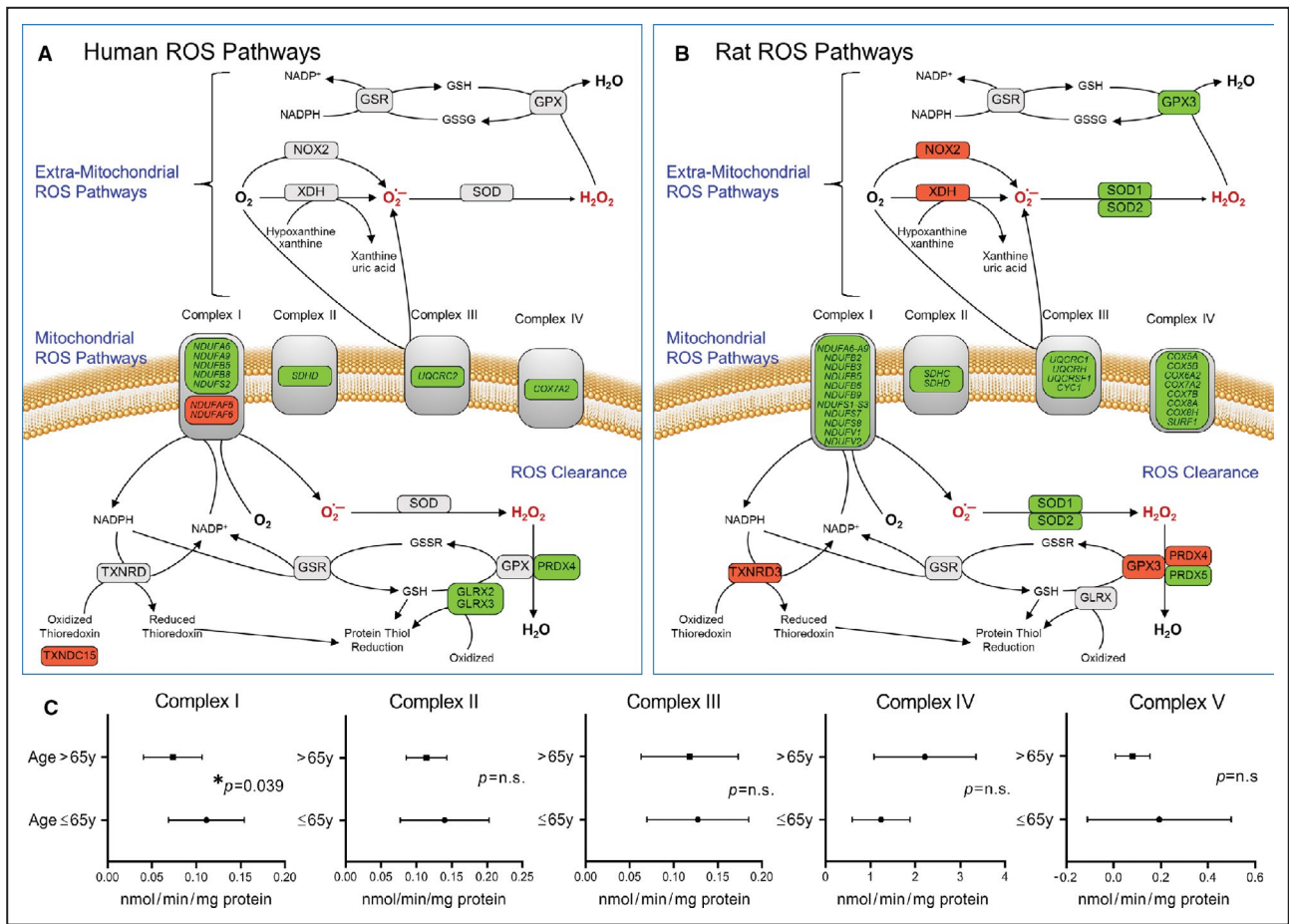
Figure 2. Differentially expressed genes associated with mitochondrial and extramitochondrial ROS metabolism pathways.
Transcriptomic changes in genes associated with ROS metabolism (ROS production and clearance) in aged human and rat hearts compared to adults (detail annotations found in Table S4). Shown here is a schematic representation of ROS production and clearance pathways, highlighting the genes in (**A**) aged human atria and (**B**) aged rat myocardium that are significantly upregulated (red) and downregulated (green) when compared to adult hearts. Genes that show no change in expression are depicted in gray. **C**, Functional activities of mitochondrial complexes as an indicator of oxidative phosphorylation in human atrial tissue of adult (age 18–65 years) and elderly (aged >65 years) patients with well-preserved atrial and ventricular function who underwent open heart surgery. Data are expressed as nmol/min/mg protein and presented as mean±standard deviation. Complex I (n=11 for adults and n=25 for elderly), Complex II (n=9 for adults and n=25 for elderly), Complex III (n=5 for adults and n=10 for elderly), Complex IV (n=12 for adults and n=10 for elderly), and Complex V (n=11 for adults and n=25 for elderly) comparison of the adult and elderly groups was performed using t test, with significance set at $P<0.05$. ROS indicates reactive oxygen species.

Age-Dependent Changes in Expression of Selected Genes Involved in ROS Metabolism in the Human Heart

ROS metabolism-associated genes in the aged versus adult human heart showed that most of the genes that are differentially expressed with aging are localized to the mitochondria (Table S4). To define the effect of age on the mRNA expression of selected ROS production and clearance pathway genes in the human heart, qPCR was used to analyze myocardial tissue from patients ages 45 to 83 years who underwent open-heart surgery. The mitochondrial complex I subunit *NDUFA6*, which was significantly reduced in both aged human and rat hearts in microarray analysis, demonstrated a highly significant inverse correlation ($R^2=0.4059$;

$P=0.008$) in expression with advancing age (Figure 3A). In individuals older than 65 years, the total mRNA expression of mitochondrial complex I subunit *NDUFA6* was reduced −0.6-fold compared to the younger age group (Figure 3A inset). NADPH oxidase 2 (NOX2), a major extramitochondrial source for ROS production, showed no significant alteration between those older or younger than 65 years (Figure 3B). For the ROS clearance pathway, the expression of TXN2, a redox-active protein that regulates ROS levels, showed an inverse relationship with advancing age ($R^2=0.3041$; $P=0.03$) (Figure 3C) with the levels reduced −0.82-fold in those 65 years or older compared to younger individuals (Figure 3C inset). In contrast, TXNRD3, which was significantly downregulated in rat hearts (Table S4), was
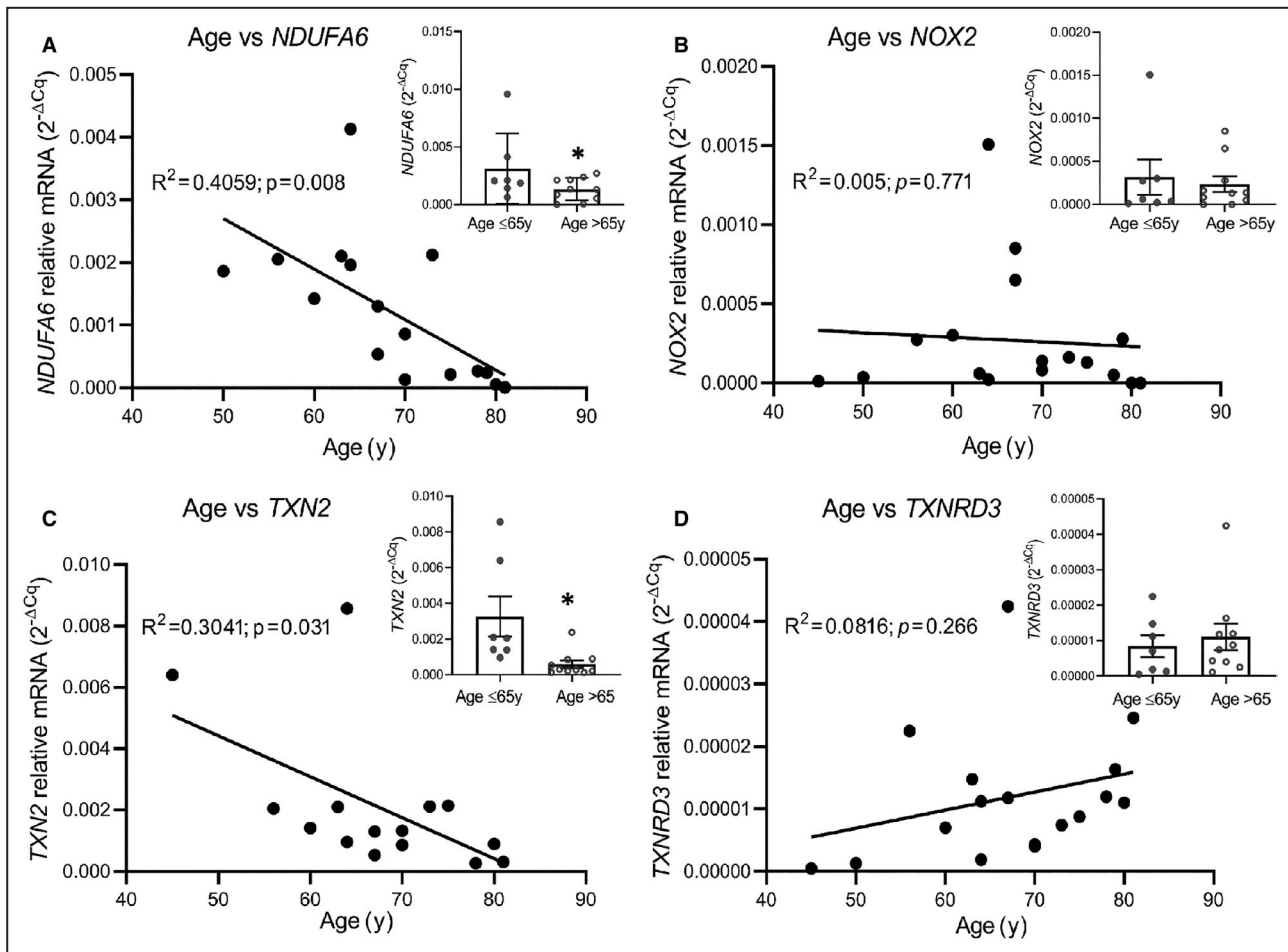
Figure 3. Assessment of expression of selected genes in human adult and aging myocardium.
Depicted are mRNA expression levels of selected genes associated with ROS metabolism in human adult (age 18–65 years, n=7) and aging (age >65 years, n=10) myocardium. **A**, Scatter plot examining age-dependent correlation of age and mRNA gene expression reveals significant inverse correlation in age vs *NDUFA6* (R^2=0.41), with total mRNA expression values from adult and elderly patients. Bars highlighting distribution of individual gene expression values along with mean±standard deviation values for each age group (inset). **B**, Inverse correlation in age vs *NOX2* mRNA expression (R^2=0.005). Total mRNA expression shown in inset. **C**, *TXN2* (R^2=0.304) shows significant inverse correlation with age, with significant total mRNA downregulation in elderly patients compared to adults (inset). **D**, No significant correlation was seen in age vs *TXNRD3* (R^2=0.08); however, an upward trend is observed. Data were analyzed by regression analysis of the sample population (n=17), *$P<0.05$.

not significantly altered in the hearts of young and old humans (Figure 3D).

Aging Increases Superoxide ($O_2^{\cdot-}$) Production in Mitochondria from the Rat Heart

Mean $O_2^{\cdot-}$ production in isolated mitochondria from the myocardium of aged rats was 1.7-fold greater than that in young adult rats. The production of $O_2^{\cdot-}$ was 1.32±0.63 nmol/mg protein/min in aged rat hearts (n=5) compared to 0.76±0.31 nmol/mg protein/min in young adult rat hearts (n=5, P=0.001; Figure 4A). Thus, under similar experimental conditions, mitochondria from aged hearts produced 70% more $O_2^{\cdot-}$ as determined

by the SOD-inhibitable cytochrome *c* reductase assay that measures mean $O_2^{\cdot-}$ production (Figure 4A).

Aging Increases H_2O_2 Production in Isolated Cardiomyocytes in the Unstressed and Stressed States

H_2O_2 production from the isolated cardiomyocytes was measured in the unstressed state. Following 45 minutes of incubation with DCFDA, the change in fluorescence intensity was measured with a confocal microscope every minute for 10 minutes (Figure 4B). The cumulative results of five independent experiments in adult rats and aged rats are shown in the right graph in Figure 4B. Cardiomyocytes from aged
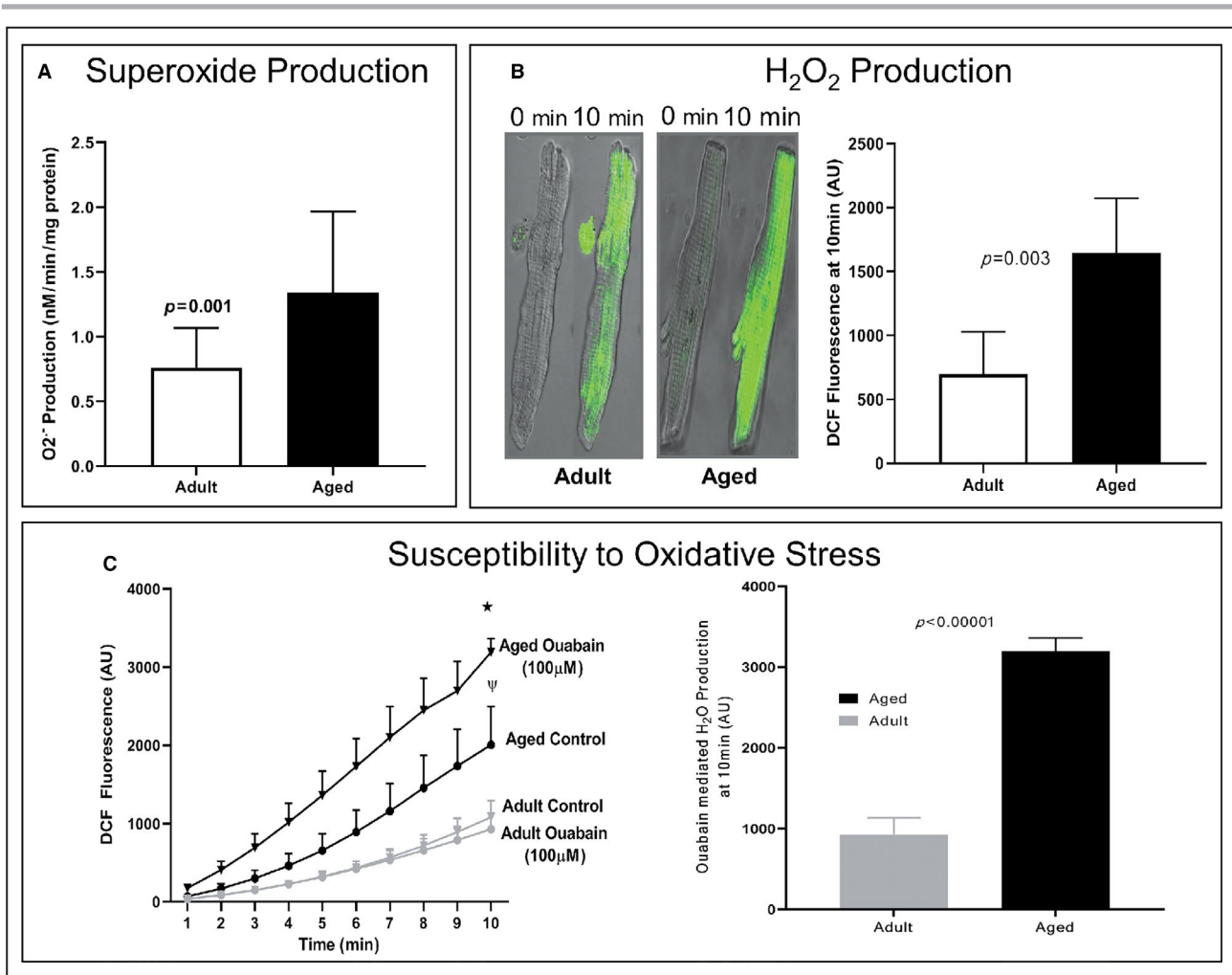
Figure 4. Rate of suppressible superoxide ($O_2^{.-}$) production in the presence of glutamate/malate substrate (5 mmol/L) in isolated mitochondria from adult and aged rat hearts.

A, Increased reduction manifests as an increase in $O_2^{.-}$ production with aging (n=19, $P<0.01$). **B**, Left panel: Age-related changes in H_2O_2 production in unstressed isolated cardiomyocytes from adult and aged rats were measured using the DCFDA assay. Shown are confocal images at 0 and 10 minutes after 45 minutes of DCFDA pre-incubation. Right Panel: DCFDA quantification exhibits a significant increase in fluorescence in unstressed cardiac cells isolated from aged animals (n=5 adult vs n=5 aged rats, $P=0.003$). **C**, Time-dependent increase in DCFDA fluorescence in aged cardiomyocytes compared to that of adult cardiomyocytes with or without reactive oxygen species (ROS) production stimulated by 100 µmol/L ouabain treatment (n=5; $*P<0.001$, $^{\psi}P<0.01$; bottom left graph). Differences in ouabain-induced fluorescence at 10 minutes between adult (6 months old) and aged (24 months old) ventricular cardiomyocytes isolated from Fischer 344 rats demonstrate a significant increase in ROS production in aged animals (bottom right).

rats produced a 2.2-fold higher level of H_2O_2 than cardiomyocytes from adult animals (1646±428 versus 699±329 arbitrary units [AU] of fluorescence, $P=0.003$) (Figure 4B). A significant time-dependent (1–10 minutes) increase in DCF fluorescence was observed in aged cardiomyocytes compared to that observed in adult cardiomyocytes without ouabain (Figure 4C, left graph). Ouabain (100 µmol/L) induced a statistically significant increase in DCF fluorescence in cardiomyocytes from aged rats (1646±428 to 3222±234, $P=0.006$) but not from adult rats (699±329 to 989±366; $P=0.17$; Figure 4C, left graph), demonstrating a 3.7-fold higher production of H_2O_2 in aged cardiomyocytes than in

adult cardiomyocytes following ouabain treatment ($P=0.00004$; Figure 4C, right graph). These differences in ouabain-induced H_2O_2 fluorescent signal at 10 minutes between adult and aged cardiomyocytes from rats indicate increased ouabain sensitivity and higher oxidative stress in aged myocardium (Figure 4C).

Aging-Related Increase in Superoxide Production and 4-HNE Protein Adducts in Human Myocardium

Mitochondrial superoxide production, as assessed by MitoSOX fluorescence in response to complex III
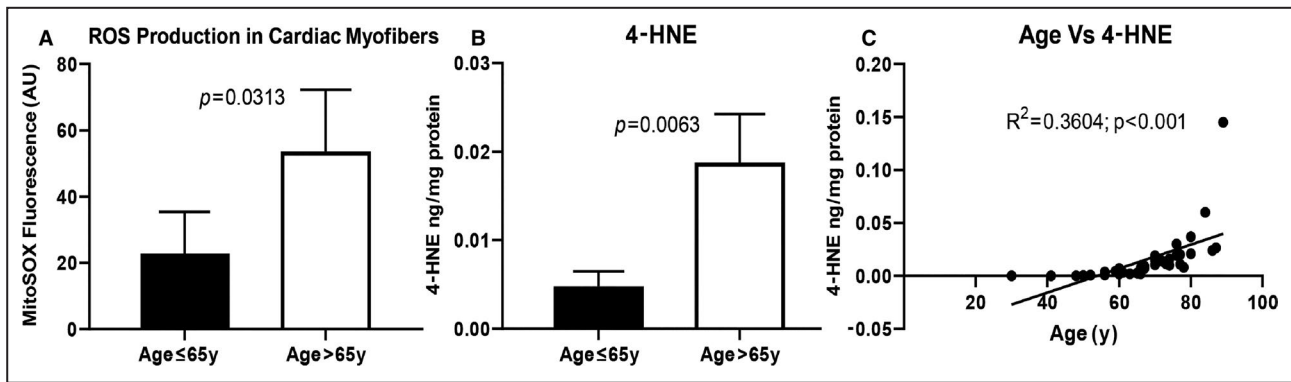
Figure 5. Difference in mitochondrial superoxide level and 4-HNE protein adducts in the adult and aged human right atrial appendages.

A, Difference in fluorescence intensity of MitoSOX Red, indicative of superoxide production in permeabilized myofibers from adult (age 18–65 years) and aged (age >65 years) right atria after antimycin A (10 μmol/L; 15 minutes) stimulation. Fibers were stained with 2.5 μmol/L MitoSOX Red (λex/λem=510/580), and fluorescence intensity was determined using laser scanning confocal fluorescence microscopy (Olympus FV1200). Data are presented as mean±standard error; n=6 for adult and n=8 for aged. Comparison of the adult and elderly groups was performed using t test, and $P<0.05$ was considered significant. **B**, Increased levels of 4-HNE were observed in aged tissue following normalization to protein concentration in tissue supernatant. Data are presented as mean±standard deviation; n=14 for adult, n=27 aged. **C**, Scatter plot demonstrating age-dependent linear regression of the levels of 4-HNE protein adduct indicative of overall lipid peroxidation in human myocardial tissue of the patient sample population (n=41) who underwent elective open-heart surgery with age.

inhibitor antimycin A, was also significantly higher in the human permeabilized myofibers isolated from aged (age >65 years) myocardium than in that from adult (age ≤65 years) myocardium (Figure 5A). The level of 4-HNE protein adducts, a marker of lipid peroxidation and oxidative stress, was also significantly increased in elderly (age >65 years) versus adult (age ≤65 years) myocardium (187.54±54.8 versus 47.83±16.7 ng/mg protein, $P=0.0063$; Figure 5B). The levels of 4-HNE protein adducts significantly correlated with increasing age ($R^2=0.36$; $P<0.001$) (Figure 5C), indicating an age-associated increase in oxidative stress and lipid peroxidation.

Aging Alters Levels of SOD1 and SOD2 in the Human Heart

The expression of SOD1 and SOD2 mRNA coding for two major superoxide scavengers superoxide dismutase (SOD) 1 and SOD2 present in the heart was downregulated in the aging rat myocardium (Table S4). In humans, immunoblots of SOD1 and SOD2 and reference protein β-tubulin in myocardium from various age groups (28–79 years) demonstrated a similar reduction in mean SOD1 protein expression ($P=0.048$) with aging but not SOD2 ($P=0.106$; Figure 6A through 6C). Overall, an inverse relationship in the expression of SOD1 protein level (a statistically significant decline) was observed with increasing age ($R^2=0.5725$; $P=0.011$; Figure 6D), which is in contrast to a higher expression

of SOD2 level with increasing age ($R^2=0.138$; $P=0.29$; Figure 6E).

Functional Network Analysis of Prioritized Genes With Aging in Human and Rat Aging-Associated Networks

Functional network analysis of the merged collective network for human and rat samples revealed common genes prioritized in human and rat aging-associated networks (Figure 7). Specifically, human samples prioritized *MYC*, *AKT*, *ERK1/2*, *P38 MAPK*, and *NFKB* complex as betweenness and closeness centrality network nodes, whereas rat samples exhibited priority of *TP53*, *MYC*, *ERK*, and *AKT* genes (Figure 7A and 7B). In addition, species-specific enrichment was observed.

Analysis of individual subnetworks that comprise the collective network for human and rat further revealed that the top prioritized network (Network 1) had identical enriched top functions for each dataset, namely "metabolic disease," "developmental disorder," and "hereditary disorder" (Figure 8). Using the Molecule Predictor Analysis module in IPA, specific genes within each subnetwork were predicted to be activated/inhibited with respect to present gene expression data (Figure 8A and 8B). Although these unique gene activation/inhibition patterns were specific for human and rat samples, there were genes common to both networks, including *ERK1/2* (predicted gene activation in both datasets), *NDUFA9*, and *NDUFA6* (Figure 8C)
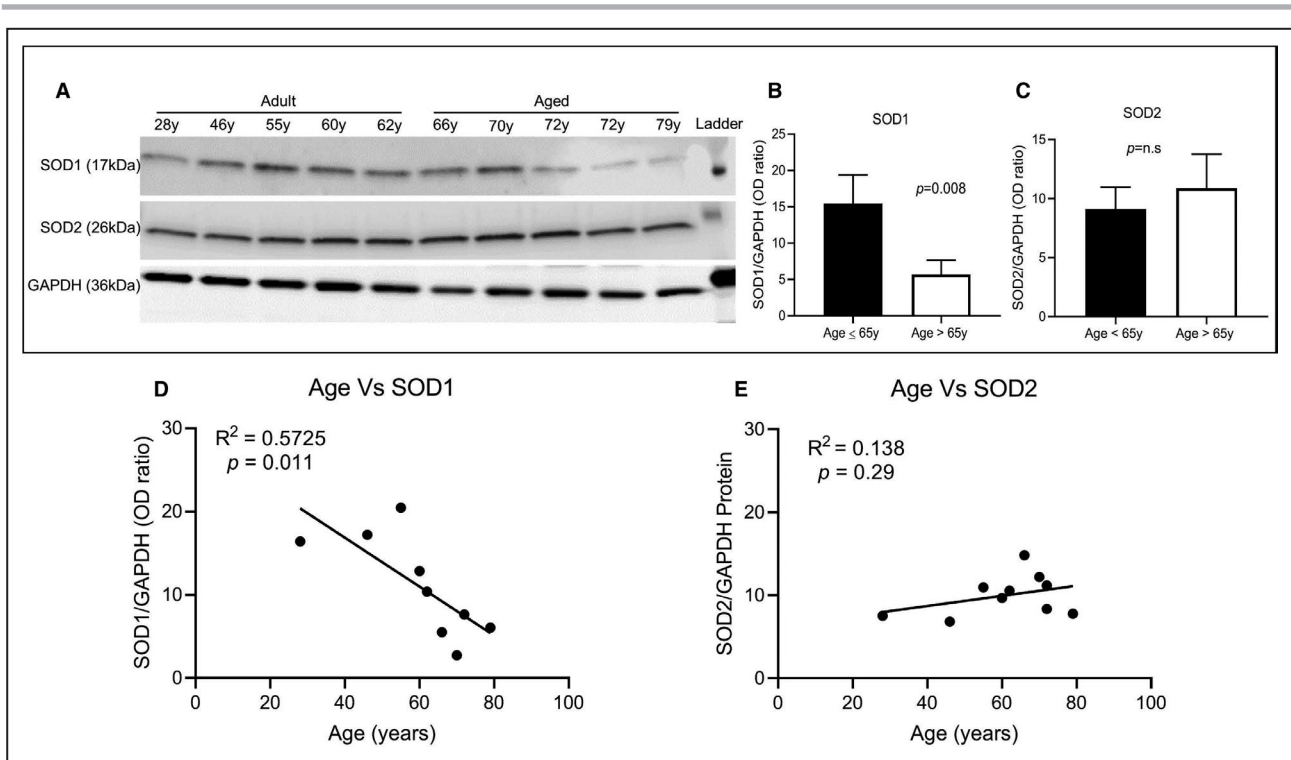
Figure 6. Age-associated changes in protein expression level of superoxide dismutase (SOD) 1 and SOD2 in human myocardium. Immunoblot data from human atrial appendage tissue lysate normalized to β-tubulin expression were analyzed in ≤65 years old and >65 years old groups.
A, Immunoblots of human atrial tissue from different-age patient tissue showed specific bands with expected molecular size of SOD1 (≈16 kDa), SOD2 (≈26 kDa), and GAPDH (≈36 kDa). **B**, There were significant decreases in SOD1 expression with increasing age, (**C**) without any significant changes observed for SOD2 between ≤65 years (n=5) and >65 years (n=5), comparison of the adult and elderly groups was performed using t test ($P<0.05$ was considered significant). **D** and **E**, Scatter plot analysis of age vs protein expression showed a negative correlation for SOD1 ($R^2=0.5725$), whereas SOD2 ($R^2=0.138$) exhibited a positive correlation.

which underlay enriched functional terms of NADH dehydrogenase and mitochondrial complex I.

DISCUSSION

The main findings of our study are that with aging in both human and rat hearts there are alterations in the expression of genes coding for proteins involved in ROS production and clearance pathways and that selective downregulation is seen in genes encoding for mitochondrial ETC complex I and III sites of ROS production in rat mitochondria but only for complex I in human myocardium. In the extramitochondrial ROS generation pathway, mRNA expression of both *XDH* and *NOX2* was upregulated in rats but not in the human heart. The gene expression changes were correlated with the reduction in functional activities of ETC complex I but not with other complexes. These changes were associated with enhanced ROS production in the aged myocardium in both humans and rats, as demonstrated by enhanced superoxide production and lipid peroxidation product in the human heart and increased H_2O_2 production in the aged rat heart

at baseline and with metabolic stress in isolated cardiac myocytes. Network analysis of the transcriptome highlights the critical elements involved with aging and the downstream effect of gene alteration on functional pathways, hinting at a possible linkage between complex I dysregulation and the ERK1/2 signaling pathway in the aging heart.

Aging-related mitochondrial changes and reduced myocardial functional reserves affect the heart's physiological function and responsiveness to stress[14]; however, the molecular basis for this is not entirely understood. In the present study, we showed that steady-state O_2^{--} and H_2O_2 production were significantly increased in aged animals compared to adult counterparts. In addition, the oxidant responsiveness to stress induced by ouabain exposure was well tolerated in the adult cardiomyocytes but not in cardiomyocytes from the aged animal. Similar differences in susceptibility to superoxide production with antimycin exposure were present in permeabilized myofibers from human aged myocardium but not adult. This was also reflected in a 3.8-fold higher level of 4-HNE protein adduct, a marker of lipid peroxidation product, in
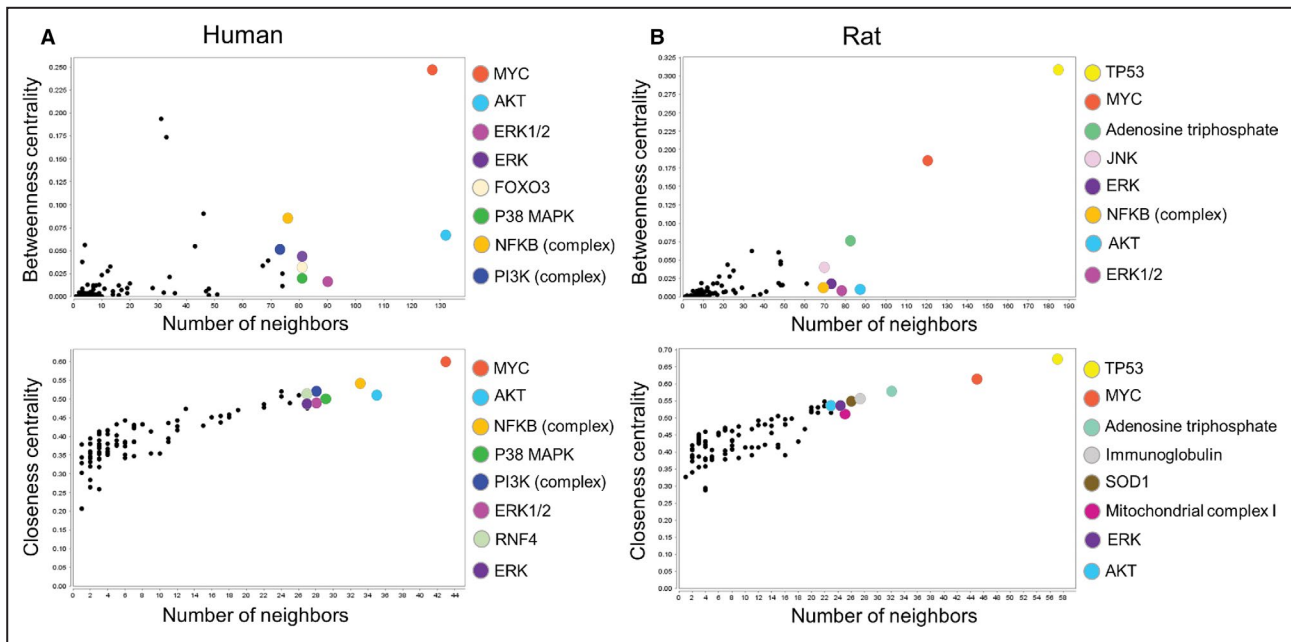
Figure 7. Cell proliferation and differentiation pathways genes are prioritized targets in the aging heart in association with reactive oxygen species (ROS).

A, Merged networks from human ROS data in aged hearts show prioritized nodes with high betweenness centrality (*MYC*, *AKT*, *ERK1/2*, *ERK*, *FOXO3*, *P38 MAPK*, NFKB [complex], and PI3K [complex]) and high closeness centrality (*MYC*, *AKT*, NFKB [complex], *P38 MAPK*, PI3K [complex], *ERK1/2*, *RNF4*, and *ERK*). **B**, Rat merged networks identified prioritized nodes with high betweenness centrality (*TP53*, *MYC*, adenosine triphosphate, *JNK*, *ERK*, NFKB [complex], *AKT*, and *ERK1/2*) and high closeness centrality (*TP53*, *MYC*, adenosine triphosphate, immunoglobulin, *SOD1*, mitochondrial complex I, *ERK*, and *AKT*).

myocardium from humans 65 years and older compared to that from younger individuals. The increased susceptibility to oxidant production in the aging heart was associated with differential expression of genes involved in ROS production and clearance as revealed by transcriptome profiling in both a rat model of aging and humans. This suggests that aging-associated enhanced susceptibility to oxidative stress is related to changes in ROS production and clearance independent of species or organism lifespan. The common link in ROS production in both species was the selective downregulation in the activity of ETC complex I involved in superoxide generation. NDUFA6 and NDUFA9 ETC subunits, and NDUFAF5 and NDUFAF6, the assembly factors of complex I, were identified as the prioritized molecules that may underlie the aging-associated reductions in mitochondrial OXPHOS efficiency and an enhanced tendency to produce superoxide within mitochondria in both species. Thus, our data indicate that similar mechanisms and pathways are involved in aging rats and humans, independent of differences in longevity, food consumption, and lifestyle.

Age-associated increased susceptibility to oxidative stress has been shown to underlie myocardial dysfunction under metabolic stress.[6,14] Low levels of $O_2^{.-}$ and H_2O_2 continuously generated as part of the normal metabolic process are essential for the maintenance

of physiological cellular function; however, excessive oxidant production becomes detrimental, resulting in myocardial dysfunction and promoting cell injury after metabolic stress such as ischemia/reperfusion.[1-4,28,29] Both cytosolic NADPH oxidase 2 and mitochondrial ETC are ROS generation sites within the cardiac myocyte, but the relative contribution to aging-associated dysfunction is not fully defined.[30] The present study recapitulated the enhanced sensitivity of ROS production in myocytes/myofibers from the aging heart and identified key elements regulating ROS synthesis and ROS clearance pathways that were differentially expressed, providing evidence for compounded impairment of ROS metabolism with aging.[31-33] Genes encoding for proteins involved in the ROS clearance cluster belong to several enzyme classes, including oxide dismutases, glutathione transferases, and oxidoreductases, and were significantly downregulated in rat and human hearts but with significant variability, which may be due to species differences or be the result of other factors related to differences in longevity, diet, or intrinsic differences in heart rate and level of stress between the two species.[6,13,14,24,28,29,31,34]

Furthermore, the results from our functional network analysis highlight a possible downstream effect among dysregulation of complex I of the mitochondrial ETC, production of ROS, and the activation of the ERK1/2
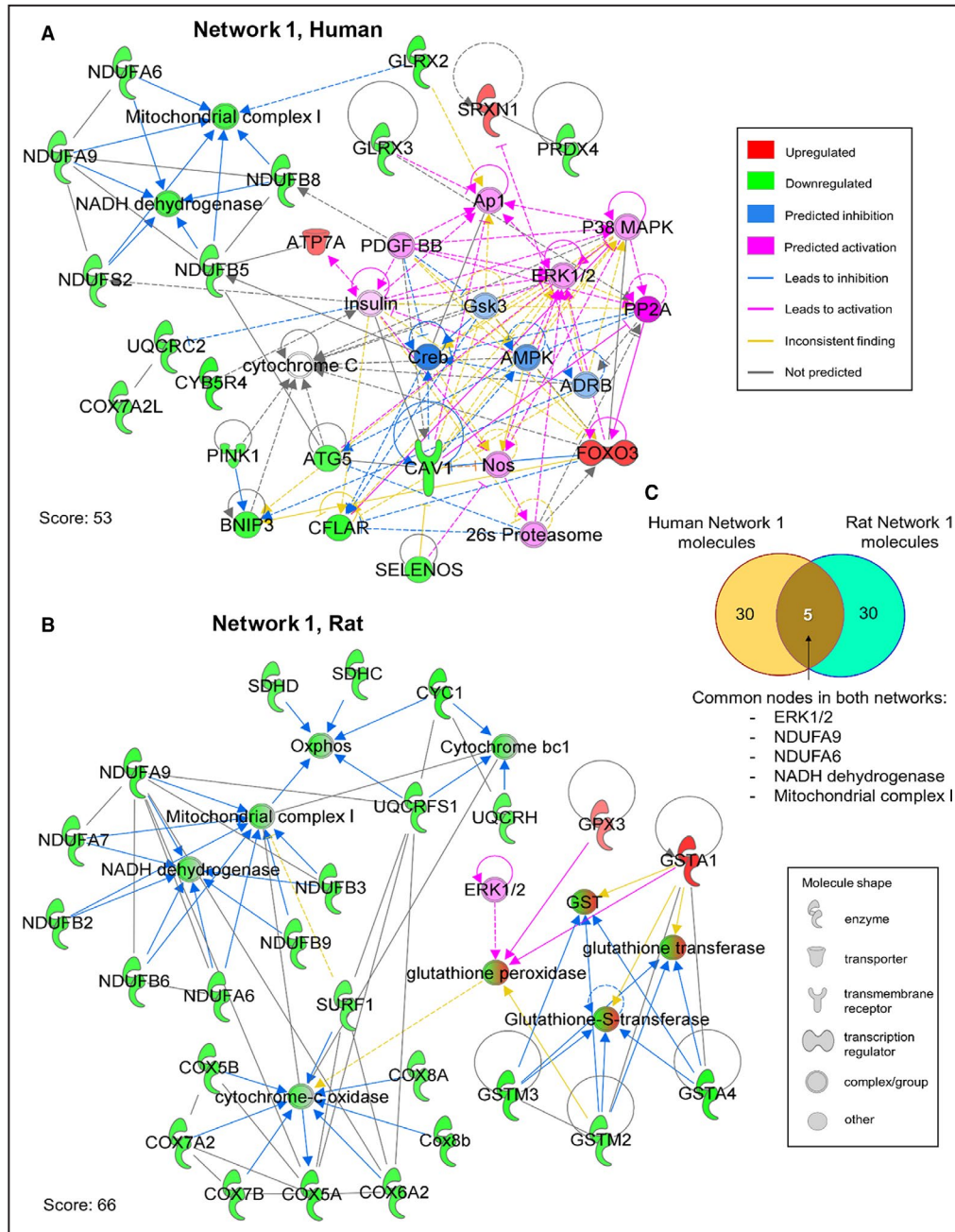
Figure 8. **Prediction of ERK1/2 pathway activation as a response to downregulation of mitochondrial complex I in the aged heart.**

Molecule predictor (MP) analysis in IPA was used to analyze the highest priority network from reactive oxygen species-related genes in aging hearts. **A**, MP analysis of IPA Network 1 in the human dataset (Score 53, top functions: metabolic disease, developmental disorder, hereditary disorder) predicted activation of *PP2A*, *P38 MAPK*, *ERK1/2*, *PDGF BB*, insulin, *AP1*, *NOS*, and the 26S proteasome as a consequence of net gene expression dynamics. *CREB*, *AMPK*, *ARDB*, and *GSK3* were predicted to be inhibited. Color and molecule shape indicated in legends. **B**, MP analysis of Network 1 from the rat dataset (Score 66, top functions: metabolic disease, developmental disorder, hereditary disorder) showed only one molecule that predicted activation, *ERK1/2*, which predicted indirect activation of glutathione peroxidase. **C**, Venn diagram highlights common nodes in both networks (five nodes), namely: *ERK1/2*, *NDUFA9*, *NDUFA6*, NADH dehydrogenase, and mitochondrial complex I.

signaling pathway in the aging heart. ROS has been implicated in the pathogenesis of heart failure, specifically in the stimulation of cardiac hypertrophy, where

H_2O_2-promoted cardiac hypertrophy has been shown to be attributed to activation of the ERK1/2 signaling pathway.[2,35-39] Ischemia-reperfusion, neurohormones,

exercise, comorbidities such as diabetes mellitus and others, and metabolic stressors can enhance the sensitivity of ROS production in the aging heart.[24,30,33,40] In the present study, we used ouabain as a mild pharmacologic stressor to identify cardiomyocytes' heightened sensitivity to H_2O_2 production in the aged rat heart and a negligible effect in cardiomyocytes from adult rats.

The effect of aging on the genomic profile of enzymatic pathways of ROS generation and clearance has not been fully characterized in the human heart. Mitochondria are the primary source of ROS production in the heart and, conversely, are most vulnerable to oxidative damage, leading to a vicious cycle of ever-increasing ROS production and dysfunctional mitochondrial damage with age.[41] Several lines of evidence support age-related decline in cardiac mitochondrial oxidative phosphorylation, mitochondrial ETC complexes, and ATP synthase.[6,8,14,15] Previously, we and others showed transcriptional downregulation of genes encoding subunits of mitochondrial ETC complexes[8,14,42,43] that contribute to the decrease in the activity and efficiency of mitochondria under metabolic and oxidative stress[6,14,44-46] as well as disease conditions reminiscent of aging, such as atrial fibrillation and heart failure in humans.[6,47] In our previous study,[14] we demonstrated that among all five OXPHOS complexes, complex I was predominantly affected by aging at the gene and protein expression level in human cardiac tissue. This was associated with a decline in the functional activity of complex I. Similarly, our group has shown an aging-related decline in complex I subunits and activity level in rat myocardium.[8] In hearts from aging rats, several complex V subunits were also downregulated, with a significant reduction in functional activity compared to adults. The main differences between the adult and aged hearts that are common between rats and humans were in complex I subunit expression and activity (Table S1), with no significant change in complex V or other OXPHOS complexes observed in adult and aged humans compared to rats. This suggests that distinctions exist related to species, overall longevity variances, different metabolic demands with marked variances in heart rate, and other physiological processes, along with possible confounding effects of comorbidities in humans not experienced by animals free of other illnesses. Moreover, these changes in mitochondrial respiratory capacity reduction could be related to aging-associated alteration in complex I activity or supercomplex destabilization as suggested by Gomez et al.[48] The loss of supercomplexes can compromise stoichiometries of OXPHOS complexes I, III, and IV as previously demonstrated in aged rats,[49] which makes electron flux through the ETC inefficient, reducing mitochondrial energetic reserve as reported by other studies.[48,50]

Differences in the expression of genes coding for the main extramitochondrial and mitochondrial sites of ROS production between the aged and adult rat and human hearts were observed. A 40% to 60% upregulation of expression of subunits of NADPH oxidase 2 (*NOX2*) and xanthine oxidoreductase (*XOR*) genes of extramitochondrial ROS production in aged rats was seen compared to adults, along with subunits of mitochondrial ETC complexes I and III. The expression of *NOX2* and *XOR* in humans remained unchanged between the adult and aged myocardium, in which the changes were mainly confined to the major mitochondrial site of ROS production within ETC complex I. The ROS clearance pathways also showed a differential effect of aging on transcripts level, downregulated by 20% to 60% in aged hearts compared to adult hearts ($P<0.02$). These changes were observed specifically in genes *SOD1*, *SOD2*, *GSTA4*, *GSTM2*, *GSTM3*, *TXN2*, *TXNDC4*, *TXNDC9*, and *PRDX5*, which code for, respectively, SOD1 and SOD2, glutathione S-transferase A4, M2 and M3, thioredoxin 2, thioredoxin domain containing 4 and 9, and peroxiredoxin 5. Overall, this suggests an aging-associated change that predisposes to higher ROS levels and a more exaggerated response to stress, with attenuation of antioxidant mechanisms. A compensatory upregulation (20–260%) of transcripts *GPX3*, *GSTA1*, *TXNRD3*, and *PRDX4*—coding for glutathione peroxidase 3, glutathione S-transferase A1, thioredoxin reductase 3, and peroxiredoxin 4, respectively, all involved in ROS clearance—was observed with aging, which may help reduce oxidant levels. The downregulated expression of both *SOD1* (predominantly localized in the cytosol but also mitochondria) and *SOD2* (localized within mitochondria) in rat hearts indicates that the dismutation of $O_2^{\cdot-}$ is altered at both of these sites.[51] These changes in *SOD1* and *SOD2* transcripts present in the aging rat model were not observed in human aged hearts, in which only protein expression of SOD1 was significantly downregulated and inversely correlated with age. The level of SOD2 proteins in the human heart was increased with aging and may represent a compensatory mechanism for countering the oxidative stress caused by increased mitochondrial $O_2^{\cdot-}$ production. These findings suggest that individual components of oxidant production and clearance may be affected differentially with aging in humans compared to animal models and may need to be further characterized to identify targets to reduce oxidative stress and maintain the redox homeostasis with aging. The glutathione peroxidases GPx2, GPx3, GPx4-7 associated with glutathione peroxidase (GPx1), which offers protection against myocardial ischemia-reperfusion injury,[52,53] were upregulated, akin to earlier observations.[54,55] Thioredoxin and thioredoxin reductases are important components of the

cellular antioxidant system involved in ROS scavenging and regulation of cell survival and cell death,[56] and in this study transcript levels of *Txnrd3* were upregulated in aging rats. GPx3 and Txnrd3 belong to the group of redox enzymes that contain catalytically active selenocysteine (SEC) residues.[57,58] The increase in expression of *GPX3* and *TXNRD3* is thus notable since the majority of ROS scavengers were either downregulated or showed no significant change in expression. This suggests that enzymes with SEC residues may serve as a secondary layer of protection in response to increased oxidative stress, activated when the primary line of defense, the mitochondrial antioxidant enzyme system against ROS generation, becomes compromised with aging. Indeed, the concept of genetic regulation of ROS production and clearance with age is strongly supported by caloric restriction experiments that demonstrated how transcriptional reprogramming of gene sets leads to overall oxidative stress reduction.[59] Concisely, the reduced expression of important components of these protective pathways in the aging heart in both rats and humans highlights a common mechanism underlying the reduced capacity of the aged heart to counter oxidative stress that, in turn, increases predisposition to myocardial injury under stress, as well as promotion of interstitial fibrosis and overall myocardial dysfunction.[60,61]

The main limitation of the study is that the observed changes in the levels of individual transcripts were small (20% to 60%); however, the cumulative effect of these changes in the ROS production and clearance pathways could have a significant impact on the aging-associated susceptibly to oxidative stress and myocardial dysfunction.[60]

Clinical Implication

In summary, our findings suggest that aging influences both mitochondrial and extramitochondrial pathways of ROS production and clearance within the myocardium, disbalancing the oxidant and antioxidant system, promoting a higher level of oxidants under steady-state conditions, and, in response to metabolic stress with significant downstream effects, promoting a higher susceptibility to injury. ROS-mediated activation of the ERK1/2 pathway identified in network analysis warrants further studies; recognizing components of ROS homeostasis regulators and downstream players altered by aging may identify targets that can be selectively intervened on to prevent aging-associated electrical or mechanical myocardial dysfunction, such as atrial fibrillation and heart failure, prevalent in the elderly.

ARTICLE INFORMATION

Affiliations

Center for Integrative Research on Cardiovascular Aging (CIRCA), Aurora Research Institute, Milwaukee, WI (F.R., L.E., G.R.R., E.L.H., A.J.); Division of Cardiovascular Diseases, Department of Medicine, Mayo Clinic Rochester, Rochester, MN (C.C.P., M.V., A.J.); Genetics and Genomics Group, Sanford Research, Sioux Falls, SD (C.C.P., R.S.F.); Department of Internal Medicine, Mayo Clinic Health System, Austin, MN (M.Y.); Quality Management, Advocate Aurora Health, Milwaukee, WI (O.D.); Now with Institute of Theoretical and Experimental Biophysics, Russian Academy of Sciences, Pushchino, Russian Federation (E.L.H.); and Center for Advanced Atrial Fibrillation Therapies, Advocate Aurora Health, Milwaukee, WI (O.D., A.J.).

Disclosures

None.

Supplementary Material

Tables S1–S4

REFERENCES

1. Fridovich I. Chairman's introduction. In: Fitzsimons DW, ed. Ciba Foundation Symposium 65 - Oxygen Free Radicals and Tissue Damage. *Amsterdam: Excerpta Medica*. 1979;65:1–4.

2. Nishida M, Maruyama Y, Tanaka R, Kontani K, Nagao T, Kurose H. G alpha(i) and G alpha(o) are target proteins of reactive oxygen species. *Nature*. 2000;408:492–495.

3. Oldenburg O, Cohen MV, Downey JM. Mitochondrial K(ATP) channels in preconditioning. *J Mol Cell Cardiol*. 2003;35:569–575. DOI: 10.1016/S0022-2828(03)00115-9.

4. Orrenius S, Gogvadze V, Zhivotovsky B. Mitochondrial oxidative stress: implications for cell death. *Annu Rev Pharmacol Toxicol*. 2007;47:143–183. DOI: 10.1146/annurev.pharmtox.47.120505.105122.

5. Forman DE, Arena R, Boxer R, Dolansky MA, Eng JJ, Fleg JL, Haykowsky M, Jahangir A, Kaminsky LA, Kitzman DW, et al. Prioritizing functional capacity as a principal end point for therapies oriented to older adults with cardiovascular disease: a scientific statement for healthcare professionals from the American Heart Association. *Circulation*. 2017;135:e894–e918. DOI: 10.1161/CIR.0000000000000483.

6. Emelyanova L, Ashary Z, Cosic M, Negmadjanov U, Ross G, Rizvi F, Olet S, Kress D, Sra J, Tajik AJ, et al. Selective downregulation of mitochondrial electron transport chain activity and increased oxidative stress in human atrial fibrillation. *Am J Physiol Heart Circ Physiol*. 2016;311:H54–H63. DOI: 10.1152/ajpheart.00699.2015.

7. Gredilla R, Sanz A, Lopez-Torres M, Barja G. Caloric restriction decreases mitochondrial free radical generation at complex I and lowers oxidative damage to mitochondrial DNA in the rat heart. *FASEB J*. 2001;15:1589–1591. DOI: 10.1096/fj.00-0764fje.

8. Preston CC, Oberlin AS, Holmuhamedov EL, Gupta A, Sagar S, Syed RH, Siddiqui SA, Raghavakaimal S, Terzic A, Jahangir A. Aging-induced alterations in gene transcripts and functional activity of mitochondrial oxidative phosphorylation complexes in the heart. *Mech Ageing Dev*. 2008;129:304–312. DOI: 10.1016/j.mad.2008.02.010.

9. Ping P, Gustafsson ÅB, Bers DM, Blatter LA, Cai H, Jahangir A, Kelly D, Muoio D, O'Rourke B, Rabinovitch P, et al. Harnessing the power of integrated mitochondrial biology and physiology: a special report on the NHLBI mitochondria in heart diseases initiative. *Circ Res*. 2015;117:234–238. DOI: 10.1161/CIRCRESAHA.117.306693.

10. Nemutlu E, Gupta A, Zhang S, Viqar M, Holmuhamedov E, Terzic A, Jahangir A, Dzeja P. Decline of phosphotransfer and substrate supply metabolic circuits hinders ATP cycling in aging myocardium. *PLoS One*. 2015;10:e0136556. DOI: 10.1371/journal.pone.0136556.

11. Sohal RS. Aging, cytochrome oxidase activity, and hydrogen peroxide release by mitochondria. *Free Radic Biol Med*. 1993;14:583–588. DOI: 10.1016/0891-5849(93)90139-L.

12. Drew B, Phaneuf S, Dirks A, Selman C, Gredilla R, Lezza A, Barja G, Leeuwenburgh C. Effects of aging and caloric restriction on mitochondrial energy production in gastrocnemius muscle and heart. *Am J Physiol Regul Integr Comp Physiol*. 2003;284:R474–R480. DOI: 10.1152/ajpregu.00455.2002.

13. Zahn JM, Poosala S, Owen AB, Ingram DK, Lustig A, Carter A, Weeraratna AT, Taub DD, Gorospe M, Mazan-Mamczarz K, et al. AGEMAP: a gene expression database for aging in mice. *PLoS Genet*. 2007;3:e201. DOI: 10.1371/journal.pgen.0030201.

14. Emelyanova L, Preston C, Gupta A, Viqar M, Negmadjanov U, Edwards S, Kraft K, Devana K, Holmuhamedov E, O'Hair D, et al. Effect of aging on mitochondrial energetics in the human atria. *J Gerontol A Biol Sci Med Sci*. 2018;73:608–616. DOI: 10.1093/gerona/glx160.

15. Jahangir A, Sagar S, Terzic A. Aging and cardioprotection. *J Appl Physiol*. 2007;103:2120–2128. DOI: 10.1152/japplphysiol.00647.2007.

16. Campbell SG, Haynes P, Kelsey Snapp W, Nava KE, Campbell KS. Altered ventricular torsion and transmural patterns of myocyte relaxation precede heart failure in aging F344 rats. *Am J Physiol Heart Circ Physiol*. 2013;305:H676–H686. DOI: 10.1152/ajpheart.00797.2012.

17. Margiocco ML, Borgarelli M, Musch TI, Hirai DM, Hageman KS, Fels RJ, Garcia AA, Kenney MJ. Effects of combined aging and heart failure on visceral sympathetic nerve and cardiovascular responses to progressive hyperthermia in F344 rats. *Am J Physiol Regul Integr Comp Physiol*. 2010;299:R1555–R1563. DOI: 10.1152/ajpregu.00434.2010.

18. Xu K, Puchowicz MA, LaManna JC. Aging effect on post-recovery hypofusion and mortality following cardiac arrest and resuscitation in rats. *Adv Exp Med Biol*. 2016;876:265–270. DOI: 10.1007/978-1-4939-3023-4_33.

19. Turturro A, Witt WW, Lewis S, Hass BS, Lipman RD, Hart RW. Growth curves and survival characteristics of the animals used in the biomarkers of aging program. *J Gerontol A Biol Sci Med Sci*. 1999;54:B492–B501. DOI: 10.1093/gerona/54.11.B492.

20. Holmuhamedov EL, Wang L, Terzic A. ATP-sensitive K^+ channel openers prevent Ca^{2+} overload in rat cardiac mitochondria. *J Physiol*. 1999;519(Pt 2):347–360.

21. Liu XK, Yamada S, Kane GC, Alekseev AE, Hodgson DM, O'Cochlain F, Jahangir A, Miki T, Seino S, Terzic A. Genetic disruption of Kir6.2, the pore-forming subunit of ATP-sensitive K^+ channel, predisposes to catecholamine-induced ventricular dysrhythmia. *Diabetes*. 2004;53(suppl 3):S165–S168. DOI: 10.2337/diabetes.53.suppl_3.S165.

22. Jahangir A, Ozcan C, Holmuhamedov EL, Terzic A. Increased calcium vulnerability of senescent cardiac mitochondria: protective role for a mitochondrial potassium channel opener. *Mech Ageing Dev*. 2001;122:1073–1086. DOI: 10.1016/S0047-6374(01)00242-1.

23. Dzeja PP, Bast P, Ozcan C, Valverde A, Holmuhamedov EL, Van Wylen DG, Terzic A. Targeting nucleotide-requiring enzymes: implications for diazoxide-induced cardioprotection. *Am J Physiol Heart Circ Physiol*. 2003;284:H1048–H1056. DOI: 10.1152/ajpheart.00847.2002.

24. Boveris A. Determination of the production of superoxide radicals and hydrogen peroxide in mitochondria. *Methods Enzymol*. 1984;105:429–435.

25. Frezza C, Cipolat S, Scorrano L. Organelle isolation: functional mitochondria from mouse liver, muscle and cultured fibroblasts. *Nat Protoc*. 2007;2:287–295. DOI: 10.1038/nprot.2006.478.

26. Anderson EJ, Efird JT, Davies SW, O'Neal WT, Darden TM, Thayne KA, Katunga LA, Kindell LC, Ferguson TB, Anderson CA, et al. Monoamine oxidase is a major determinant of redox balance in human atrial myocardium and is associated with postoperative atrial fibrillation. *J Am Heart Assoc*. 2014;3:e000713. DOI: 10.1161/JAHA.113.000713.

27. Wang L, Duan Q, Wang T, Ahmed M, Zhang N, Li Y, Li L, Yao X. Mitochondrial respiratory chain inhibitors involved in ROS production induced by acute high concentrations of iodide and the effects of SOD as a protective factor. *Oxid Med Cell Longev*. 2015;2015:217670. DOI: 10.1155/2015/217670.

28. Chabi B, Ljubicic V, Menzies KJ, Huang JH, Saleem A, Hood DA. Mitochondrial function and apoptotic susceptibility in aging skeletal muscle. *Aging Cell*. 2008;7:2–12. DOI: 10.1111/j.1474-9726.2007.00347.x.

29. Southorn PA, Powis G. Free radicals in medicine. II. Involvement in human disease. *Mayo Clin Proc*. 1988;63:390–408. DOI: 10.1016/S0025-6196(12)64862-9.

30. Kornfeld OS, Hwang S, Disatnik MH, Chen CH, Qvit N, Mochly-Rosen D. Mitochondrial reactive oxygen species at the heart of the matter:

31. Gao X-H, Qanungo S, Pai HV, Starke DW, Steller KM, Fujioka H, Lesnefsky EJ, Kerner J, Rosca MG, Hoppel CL, et al. Aging-dependent changes in rat heart mitochondrial glutaredoxins–implications for redox regulation. *Redox Biol*. 2013;1:586–598. DOI: 10.1016/j.redox.2013.10.010.

32. Zhu J, Rebecchi MJ, Glass PS, Brink PR, Liu L. Cardioprotection of the aged rat heart by GSK-3beta inhibitor is attenuated: age-related changes in mitochondrial permeability transition pore modulation. *Am J Physiol Heart Circ Physiol*. 2011;300:H922–H930. DOI: 10.1152/ajpheart.00860.2010.

33. Boengler K, Schulz R, Heusch G. Loss of cardioprotection with ageing. *Cardiovasc Res*. 2009;83:247–261. DOI: 10.1093/cvr/cvp033.

34. Sawada M, Carlson JC. Changes in superoxide radical and lipid peroxide formation in the brain, heart and liver during the lifetime of the rat. *Mech Ageing Dev*. 1987;41:125–137. DOI: 10.1016/0047-6374(87)90057-1.

35. Mallat Z, Philip I, Lebret M, Chatel D, Maclouf J, Tedgui A. Elevated levels of 8-iso-prostaglandin F2alpha in pericardial fluid of patients with heart failure: a potential role for in vivo oxidant stress in ventricular dilatation and progression to heart failure. *Circulation*. 1998;97:1536–1539.

36. Dey S, DeMazumder D, Sidor A, Foster DB, O'Rourke B. Mitochondrial ROS drive sudden cardiac death and chronic proteome remodeling in heart failure. *Circ Res*. 2018;123:356–371. DOI: 10.1161/CIRCRESAHA.118.312708.

37. Sugden PH, Clerk A. Oxidative stress and growth-regulating intracellular signaling pathways in cardiac myocytes. *Antioxid Redox Signal*. 2006;8:2111–2124. DOI: 10.1089/ars.2006.8.2111.

38. Kwon SH, Pimentel DR, Remondino A, Sawyer DB, Colucci WS. $H(2)O(2)$ regulates cardiac myocyte phenotype via concentration-dependent activation of distinct kinase pathways. *J Mol Cell Cardiol*. 2003;35:615–621. DOI: 10.1016/S0022-2828(03)00084-1.

39. Xiao L, Pimental DR, Amin JK, Singh K, Sawyer DB, Colucci WS. MEK1/2-ERK1/2 mediates alpha1-adrenergic receptor-stimulated hypertrophy in adult rat ventricular myocytes. *J Mol Cell Cardiol*. 2001;33:779–787.

40. Chouchani ET, Pell VR, Gaude E, Aksentijević D, Sundier SY, Robb EL, Logan A, Nadtochiy SM, Ord ENJ, Smith AC, et al. Ischaemic accumulation of succinate controls reperfusion injury through mitochondrial ROS. *Nature*. 2014;515:431–435. DOI: 10.1038/nature13909.

41. Rohrbach S, Niemann B, Abushouk AM, Holtz J. Caloric restriction and mitochondrial function in the ageing myocardium. *Exp Gerontol*. 2006;41:525–531. DOI: 10.1016/j.exger.2006.02.001.

42. Bodyak N, Kang PM, Hiromura M, Sulijoadikusumo I, Horikoshi N, Khrapko K, Usheva A. Gene expression profiling of the aging mouse cardiac myocytes. *Nucleic Acids Res*. 2002;30:3788–3794. DOI: 10.1093/nar/gkf497.

43. Yan L, Ge H, Li H, Lieber SC, Natividad F, Resuello RR, Kim SJ, Akeju S, Sun A, Loo K, et al. Gender-specific proteomic alterations in glycolytic and mitochondrial pathways in aging monkey hearts. *J Mol Cell Cardiol*. 2004;37:921–929. DOI: 10.1016/j.yjmcc.2004.06.012.

44. Lesnefsky EJ, Gudz TI, Moghaddas S, Migita CT, Ikeda-Saito M, Turkaly PJ, Hoppel CL. Aging decreases electron transport complex III activity in heart interfibrillar mitochondria by alteration of the cytochrome c binding site. *J Mol Cell Cardiol*. 2001;33:37–47. DOI: 10.1006/jmcc.2000.1273.

45. Paradies G, Ruggiero FM, Petrosillo G, Gadaleta MN, Quagliariello E. Effect of aging and acetyl-L-carnitine on the activity of cytochrome oxidase and adenine nucleotide translocase in rat heart mitochondria. *FEBS Lett*. 1994;350:213–215.

46. Paradies G, Ruggiero FM, Petrosillo G, Quagliariello E. Age-dependent decline in the cytochrome c oxidase activity in rat heart mitochondria: role of cardiolipin. *FEBS Lett*. 1997;406:136–138.

47. Ide T, Tsutsui H, Kinugawa S, Utsumi H, Kang D, Hattori N, Uchida K, Arimura K, Egashira K, Takeshita A. Mitochondrial electron transport complex I is a potential source of oxygen free radicals in the failing myocardium. *Circ Res*. 1999;85:357–363. DOI: 10.1161/01.RES.85.4.357.

48. Gomez LA, Hagen TM. Age-related decline in mitochondrial bioenergetics: does supercomplex destabilization determine lower oxidative capacity and higher superoxide production? *Semin Cell Dev Biol*. 2012;23:758–767. DOI: 10.1016/j.semcdb.2012.04.002.

49. Gomez LA, Monette JS, Chavez JD, Maier CS, Hagen TM. Supercomplexes of the mitochondrial electron transport chain decline

in the aging rat heart. *Arch Biochem Biophys*. 2009;490:30–35. DOI: 10.1016/j.abb.2009.08.002.

50. Genova ML, Baracca A, Biondi A, Casalena G, Faccioli M, Falasca AI, Formiggini G, Sgarbi G, Solaini G, Lenaz G. Is supercomplex organization of the respiratory chain required for optimal electron transfer activity? *Biochim Biophys Acta*. 2008;1777:740–746. DOI: 10.1016/j.bbabio.2008.04.007.

51. Fukai T, Ushio-Fukai M. Superoxide dismutases: role in redox signaling, vascular function, and diseases. *Antioxid Redox Signal*. 2011;15:1583–1606. DOI: 10.1089/ars.2011.3999.

52. Yoshida T, Watanabe M, Engelman DT, Engelman RM, Schley JA, Maulik N, Ho YS, Oberley TD, Das DK. Transgenic mice overexpressing glutathione peroxidase are resistant to myocardial ischemia reperfusion injury. *J Mol Cell Cardiol*. 1996;28:1759–1767. DOI: 10.1006/jmcc.1996.0165.

53. Yoshida T, Maulik N, Engelman RM, Ho YS, Magnenat JL, Rousou JA, Flack JE III, Deaton D, Das DK. Glutathione peroxidase knockout mice are susceptible to myocardial ischemia reperfusion injury. *Circulation*. 1997;96:II-216–II-220.

54. Meng Q, Wong YT, Chen J, Ruan R. Age-related changes in mitochondrial function and antioxidative enzyme activity in fischer 344 rats. *Mech Ageing Dev*. 2007;128:286–292. DOI: 10.1016/j.mad.2006.12.008.

55. Panel M, Panel M, Ghaleh B, Morin D. Mitochondria and aging: a role for the mitochondrial transition pore? *Aging Cell*. 2018;17:e12793. DOI: 10.1111/acel.12793.

56. Pickering AM, Lehr M, Gendron CM, Pletcher SD, Miller RA. Mitochondrial thioredoxin reductase 2 is elevated in long-lived primate as well as rodent species and extends fly mean lifespan. *Aging Cell*. 2017;16:683–692. DOI: 10.1111/acel.12596.

57. Rayman MP. Selenium and human health. *Lancet*. 2012;379:1256–1268. DOI: 10.1016/S0140-6736(11)61452-9.

58. Kasaikina MV, Hatfield DL, Gladyshev VN. Understanding selenoprotein function and regulation through the use of rodent models. *Biochim Biophys Acta*. 2012;1823:1633–1642. DOI: 10.1016/j.bbamcr.2012.02.018.

59. Park SK, Prolla TA. Gene expression profiling studies of aging in cardiac and skeletal muscles. *Cardiovasc Res*. 2005;66:205–212. DOI: 10.1016/j.cardiores.2005.01.005.

60. Huang Q, Zhou HJ, Zhang H, Huang Y, Hinojosa-Kirschenbaum F, Fan P, Yao L, Belardinelli L, Tellides G, Giordano FJ, et al. Thioredoxin-2 inhibits mitochondrial reactive oxygen species generation and apoptosis stress kinase-1 activity to maintain cardiac function. *Circulation*. 2015;131:1082–1097. DOI: 10.1161/CIRCULATIONAHA.114.012725.

61. Kiermayer C, Northrup E, Schrewe A, Walch A, de Angelis MH, Schoensiegel F, Zischka H, Prehn C, Adamski J, Bekeredjian R, et al. Heart-specific knockout of the mitochondrial thioredoxin reductase (Txnrd2) induces metabolic and contractile dysfunction in the aging myocardium. *J Am Heart Assoc*. 2015;4:e002153. DOI: 10.1161/JAHA.115.002153.

Supplemental Material

Table S1. **Clinical Characteristics of Patients in the Study.**

Variable	Aged (≥ 65Years)	Adult (< 65 Years)	p-Value
Number of samples (n)	20	11	
Age, mean ± SD	73.0 ± 5.8	53.8 ± 9.1	
Left ventricular ejection fraction % + SD	56.9 ± 13.9	61.8 ± 7.8	0.50
	Percent (%)	Percent (%)	
Male	67	82	0.44
Hypertension	71	73	0.99
Diabetes	38	9	0.11
Hyperlipidemia	81	55	0.21
Smoking	67	55	0.70
Obesity	38	36	0.99
Obstructive sleep apnea	5	18	0.27
Chronic kidney disease	29	9	0.07
Previous myocardial infarction	19	9	0.64
Heart failure	14	46	0.09
Valve disease	52	46	0.99
Statins	62	50	0.70
ACE inhibitors/ ARBs	62	40	0.44
Beta-blocker	67	50	0.45
Calcium channel blocker	19	20	0.99
Diuretics	33	40	0.99

Table S2. **Information on gene-specific primer sequences used in this study.**

Gene Name	RefSeq ID	Entrez Gene ID	Species	Specificity	E value	Primer Sequence
CYBB / NOX2	NM_000397	1536	*Homo sapiens*	100%	0.014	F-CTCTGAACTTGGAGACAGGCAAA R-CACAGCGTGATGACAACTCCAG
TXNRD3	NM_001039783	114112	*Homo sapiens*	100%	0.036	F-AGAGGCGTCCTCTCTGGAACAT R-GCTCTCCAGAAAGACATTTTGCC
TXN2	NM_012473.4	25828	*Homo sapiens*	100%	0.036	F-GGACCTGACTTTCAAGACCGAG R-GCCACCATCTTCTCTAACCTCG
NDUFA6	NM_002490.6	4700	*Homo sapiens*	100%	0.014	F-GACGGGATAAAGTCCGAGAAATG R-CATGTGTCCGCTGCTTCCATAC
B2M	NM_004048.4	567	*Homo sapiens*	100%	0.005	F-CCACTGAAAAAGATGAGTATGCCT R-CCAATCCAAATGCGGCATCTTCA
RNA18S5	NR_003286.4	100008588	*Homo sapiens*	100%	0.014	F-ACCCGTTGAACCCCATTCGTGA R-GCCTCACTAAACCATCCAATCGG

Table S3. **Number of Patient Samples used in the Study.**

Experiment	Aged (n)	Adult (n)
Gene expression profiling	10	10
qPCR validation	10	10
Protein expression (WB)	10	10
Mitochondrial Complex I*	25	11
Mitochondrial Complex II*	25	9
Mitochondrial Complex III*	10	5
Mitochondrial Complex IV*	10	12
Mitochondrial Complex V*	25	11
4-Hydroxynonenal (HNE)	25	14

WB = western blot; * = mitochondrial enzymatic assays.

Table S4. Differentially expressed genes coding for proteins related to ROS production and clearance pathway in human and rat aging hearts.

	Gene Name	Description	Human gene data			Rat gene data		
			FC	p (Corr) value	Entrez ID	FC	p (Corr) value	Entrez ID
ROS production								
Mitochondrial	**NDUFA6**	**NADH:ubiquinone oxidoreductase subunit A6**	**-1.2**	**0.010**	**4700**	**-1.3**	**0.006**	**315167**
Complex I	NDUFA7	NADH:ubiquinone oxidoreductase subunit A7				-1.3	0.006	299643
	NDUFA8	NADH:ubiquinone oxidoreductase subunit A8				-1.3	0.001	296658
	NDUFA9	**NADH:ubiquinone oxidoreductase subunit A9**	**-1.2**	**0.031**	**4704**	**-1.4**	**<0.001**	**362440**
	NDUFB2	NADH:ubiquinone oxidoreductase subunit B2				-1.3	0.002	362344
	NDUFB3	NADH:ubiquinone oxidoreductase subunit B3				-1.3	0.002	301427
	NDUFB5	**NADH:ubiquinone oxidoreductase subunit B5**	**-1.2**	**0.047**	**4711**	**-1.3**	**0.004**	**294964**
	NDUFB6	NADH:ubiquinone oxidoreductase subunit B6				-1.3	0.001	297990
	NDUFB8	NADH:ubiquinone oxidoreductase subunit B8	-1.3	0.048	4714			
	NDUFB9	NADH:ubiquinone oxidoreductase subunit B9				-1.3	0.003	299954
	NDUFS1	NADH:ubiquinone oxidoreductase core subunit S1				-1.4	0.004	301458
	NDUFS2	**NADH:ubiquinone oxidoreductase core subunit S2**	**-1.2**	**0.049**	**4720**	**-1.3**	**0.003**	**289218**
	NDUFS3	NADH:ubiquinone oxidoreductase core subunit S3				-1.4	0.001	295923
	NDUFS7	NADH:ubiquinone oxidoreductase core subunit S7				-1.5	<0.001	362837
	NDUFS8	NADH:ubiquinone oxidoreductase core subunit S8				-1.3	0.002	293652
	NDUFV1	NADH:ubiquinone oxidoreductase core subunit V1				-1.5	<0.001	293655
	NDUFV2	NADH:ubiquinone oxidoreductase core subunit V2				-1.4	0.002	81728
	NDUFAF5	NADH:ubiquinone oxidoreductase complex assembly factor 5	1.2	0.030	79133			
	NDUFAF6	NADH:ubiquinone oxidoreductase complex assembly factor 6	1.6	0.002	137682			
Complex II	SDHC	succinate dehydrogenase complex, subunit C				-1.3	0.002	289217
	SDHD	**succinate dehydrogenase complex, subunit D**	**-1.3**	**0.038**	**6392**	**-1.2**	**0.007**	**363061**
Complex III	UQCRC1	ubiquinol-cytochrome c reductase core protein 1				-1.4	0.001	301011
	UQCRC2	ubiquinol-cytochrome c reductase core protein 2	-1.3	0.011	7385			
	UQCRH	ubiquinol-cytochrome c reductase hinge protein				-1.2	0.009	366448
	UQCRFS1	ubiquinol-cytochrome c reductase, Rieske iron-sulfur polypeptide 1				-1.3	0.002	291103
	CYC1	cytochrome c-1				-1.5	<0.001	300047
Complex IV	COX5A	cytochrome c oxidase subunit 5A				-1.4	<0.001	252934
	COX5B	cytochrome c oxidase subunit 5B				-1.3	0.002	94194
	COX6A2	cytochrome c oxidase subunit 6A2				-1.3	0.003	25278
	COX7A2	**cytochrome c oxidase subunit 7A2**	**-1.2**	**0.040**	**9167**	-1.3	0.005	298762
	COX7B	cytochrome c oxidase subunit 7B				-1.3	0.007	303393
	COX8A	cytochrome c oxidase subunit 8A				-1.2	0.009	171335
	COX8H	cytochrome c oxidase subunit 8H				-1.4	0.001	25250

Category	Symbol	Description						
	SURF1	surfeit 1, cytochrome c oxidase assembly factor				-1.2	0.001	64463
Other mitochondrial	**COQ9**	**coenzyme Q9**	**-1.4**	**0.023**	**57017**	**1.6**	**0.016**	**66021**
	CYP4X1	cytochrome P450 family 4 subfamily X member 1	1.3	0.027	260293			
Extramitochondrial	*CYBB / NOX2*	NOX2, cytochrome B-245 Beta Chain				1.6	0.016	66021
	XDH	Xanthine dehydrogenase				1.4	0.027	497811
ROS clearance								
	CYB5R4	cytochrome b5 reductase 4	-1.5	0.006	51167			
	GLRX2	glutaredoxin 2	-1.4	0.048	51022			
	GLRX3	glutaredoxin 3	-1.3	0.004	10539			
	GPX3	glutathione peroxidase type 3				1.6	0.005	64317
	GSTA1	glutathione S-transferase A3				2.6	<0.001	24421
	GSTA4	**glutathione S-transferase A4**	**-1.4**	**0.030**	**2941**	**-1.6**	**0.001**	**300850**
	GSTM2	glutathione S-transferase mu 2				-1.3	0.001	24424
	GSTM3	glutathione S-transferase mu 3				-1.5	0.028	108348148
	MARC2	mitochondrial amidoxime reducing component 2	-1.2	0.021	54996			
	OXSR1	oxidative stress responsive kinase 1	-1.3	0.024	9943			
	PRDX4	**peroxiredoxin 4**	**-1.3**	**0.031**	**10549**	**1.3**	**0.028**	**85274**
	PRDX5	peroxiredoxin 5				-1.4	0.001	113898
	SOD1	superoxide dismutase 1				-1.2	0.011	24786
	SOD2	superoxide dismutase 2				-1.4	0.017	24787
	SRXN1	sulfiredoxin 1	1.2	0.016	140809			
	TMX2	thioredoxin-related transmembrane protein 2	-1.3	0.008	51075			
	TMX4	thioredoxin-related transmembrane protein 4	-1.3	0.034	56255			
	TXN2	thioredoxin 2				-1.5	<0.001	79462
	TXNDC1	thioredoxin domain containing 1				1.3	0.013	362751
	TXNDC4	thioredoxin domain containing 4				-1.2	0.025	298066
	TXNDC9	thioredoxin domain containing 9				-1.2	0.020	280671
	TXNDC15	thioredoxin domain containing 15	1.3	0.014	79770			
	TXNRD3	thioredoxin reductase 3				2.2	0.001	297437
Other ROS metabolism								
	ARF4	ADP ribosylation factor 4	-1.4	<0.001	378			
	ATG5	autophagy related 5	-1.2	0.049	9474			
	ATP7A	ATPase copper transporting alpha	1.2	0.013	538			
	BNIP3	BCL2 interacting protein 3	-1.4	0.047	664			
	CAV1	caveolin 1	-1.4	0.002	857			
	CFLAR	CASP8 and FADD like apoptosis regulator	-1.5	0.003	8837			
	DHFR	dihydrofolate reductase	1.3	0.044	1719			
	FOXO3A	forkhead box O3	1.5	0.004	2309			
	NNT	nicotinamide nucleotide transhydrogenase	-1.6	0.006	23530			

			-1.3	0.007	5160	
PDHA1	pyruvate dehydrogenase E1 alpha 1 subunit		-1.3	0.007	5160	
PINK1	PTEN induced kinase 1		-1.3	0.049	65018	
SELENOS	selenoprotein S		-1.3	0.038	55829	

Shown are 33 mitochondrial electron transport chain (ETC)-related genes from human and rat aging hearts (as shown previously, Preston et al[8]; Emelyanova et al[14]) and 39 other extramitochondrial-related genes involved in the ROS pathway. Highlighted in bold are the genes that are changing in both datasets. FC = fold change, p (Corr) = corrected p Value, ROS = reactive oxygen species.